haematologica
Journal of the Ferrata Storti Foundation

Liver sinusoidal endothelial cells integrate metabolic and immune signals for MAPK-dependent BMP6 regulation and hepcidin induction

by Ruiyue Qiu, Stefania Cucinelli, Christina Mertens, Ana Catarina Pêgo, Silvia Colucci, Sandro Altamura, Alireza Saadatmand, Johannes Backs, Matthias W. Hentze and Martina U. Muckenthaler

Received: June 9, 2026.
Accepted: November 16, 2026.

Citation: Ruiyue Qiu, Stefania Cucinelli, Christina Mertens, Ana Catarina Pêgo, Silvia Colucci, Sandro Altamura, Alireza Saadatmand, Johannes Backs, Matthias W. Hentze and Martina U. Muckenthaler. Liver sinusoidal endothelial cells integrate metabolic and immune signals for MAPK-dependent BMP6 regulation and hepcidin induction.
Haematologica. 2026 Nov 26. doi: 10.3324/haematol.2026.301393 [Epub ahead of print]

Publisher's Disclaimer.
E-publishing ahead of print is increasingly important for the rapid dissemination of science. Haematologica is, therefore, E-publishing PDF files of an early version of manuscripts that have completed a regular peer review and have been accepted for publication.
E-publishing of this PDF file has been approved by the authors.
After having E-published Ahead of Print, manuscripts will then undergo technical and English editing, typesetting, proof correction and be presented for the authors' final approval, the final version of the manuscript will then appear in a regular issue of the journal.
All legal disclaimers that apply to the journal also pertain to this production process.

Liver sinusoidal endothelial cells integrate metabolic and immune signals for MAPK-dependent BMP6 regulation and hepcidin induction

Ruiyue Qiu[1*], Stefania Cucinelli[1,2,3*], Christina Mertens[1,4], Ana Catarina Pêgo[1,2], Silvia Colucci[1,3], Sandro Altamura[1,2], Alireza Saadatmand[4,5], Johannes Backs[4,5], Matthias W. Hentze[2,3#], Martina U. Muckenthaler[1,2,4,6#]

[1]Department of Pediatric Hematology, Oncology and Immunology, University of Heidelberg, Heidelberg, Germany

[2]Molecular Medicine Partnership Unit, University of Heidelberg, Heidelberg, Germany

[3]European Molecular Biology Laboratory, Heidelberg, Germany

[4]DZHK (German Centre for Cardiovascular Research), Partner Site Heidelberg/Mannheim, Germany

[5]Institute of Experimental Cardiology, University of Heidelberg, Heidelberg, Germany

[6]Translational Lung Research Center Heidelberg (TLRC), German Center for Lung Research (DZL), University of Heidelberg, Heidelberg, Germany

*R.Q. and S.Cu. are joint first authors.

#M.W.H. and M.U.M. are joint last authors.
Corresponding author's details: martina.muckenthaler@med.uni-heidelberg.de

Authors' contribution

R.Q., M.W.H. and M.U.M. designed the experiments; R.Q., S.Cu., A.C.P, S.Co., C.M., A.S., J.B. performed the experiments; S.Co., S.A developed experimental systems and materials; R.Q., S.Cu., M.W.H. and M.U.M. drafted the manuscript, and all authors read and reviewed the manuscript; M.W.H. and M.U.M. supervised the project.

Acknowledgment

M.U.M. acknowledges funding from the DFG (Priority Program SPP2306 and GRK2727), from the Federal Ministry of Education and Research (BMBF; NephrESA project Nr 031L0191C), M.U.M. and S.A. also acknowledge DFG-funding from FerrOs - FOR5146. S.Cu. is an associated PhD fellow of GRK2727.

Conflicts of Interest

The authors have no conflicts of interest to disclose.

Data sharing statement

The original data supporting the findings of this study are available from the corresponding author upon reasonable request.

Artificial Intelligence (AI) use declaration

AI was not used for the preparation of the current version of the manuscript.

Highlights

- DAMPs (heme and myoglobin), PAMPs (LPS) and oxidative stress activate *Bmp6* mRNA expression via the MAPK signaling pathway
- The TLR/MAPK/BMP6 regulatory axis integrates inflammatory and iron signals
- Our work uncovers a novel connection between innate immune sensing, oxidative stress and hepatic iron homeostasis

Abstract

Liver sinusoidal endothelial cells (LSECs) separate the blood from the hepatic parenchyma and thus are at the frontline as scavengers of blood-borne waste, pathogens and metabolic stimuli. LSECs are also critical for sensing systemic iron availability by controlling the synthesis of bone morphogenetic protein (BMP) 6, which is essential for hepcidin expression in hepatocytes. Hepcidin maintains systemic iron homeostasis by inhibiting dietary iron uptake and iron release from iron recycling macrophages. Hepcidin is also an acute-phase protein and its activation by inflammation requires active BMP signaling. It is incompletely understood how signals derived from inflammation, cellular damage and iron are integrated by the liver to assure adequate hepcidin expression. Here, we show that *Bmp6* expression is activated in primary LSEC cultures upon their exposure to damage-associated molecular patterns (DAMPs), such as heme and myoglobin, pathogen-associated molecular patterns (PAMPs), such as lipopolysaccharide (LPS) and Fibroblast-Stimulating Lipopeptide-1 (FSL1), or oxidative stress inducers (H_2O_2). All regulatory cues converge at the MAPK signaling pathway, although the specific signaling branches involved are stimulus-specific. Notably, *Bmp6* upregulation in LSECs in response to all signals tested is strongly enhanced by the hepatocyte secretome. As hepatocytes critically depend on active BMP/SMAD signaling to control hepcidin activation, our results reveal that multiple sources of signaling input activating *Bmp6* in LSECs and hepcidin in hepatocytes serve to determine BMP/SMAD signaling strength. Furthermore, our findings suggest that hypoferremia may represent a convergent response to inflammation, oxidative stress and cellular damage, resulting from high hepcidin levels driven by elevated *Bmp6* expression.

Introduction

Control of systemic iron homeostasis is a dynamic process that ensures adequate iron availability for cellular processes, such as oxygen transport, mitochondrial respiration or DNA synthesis, while preventing the formation of reactive oxygen species (ROS), and consequent oxidative damage and ferroptosis (1). In mammals, this balance is achieved at the systemic level by the hepcidin–ferroportin (FPN, SLC40A1) regulatory axis, that maintains iron levels within physiological limits. Hepcidin is synthesized and secreted by hepatocytes and inhibits iron fluxes via FPN from duodenal enterocytes, macrophages, and hepatocytes into the blood (1). The functioning of this hormonal axis critically depends on cellular regulatory systems that control the expression levels of hepcidin. A fundamental and incompletely understood question is how the liver integrates signals derived from inflammation, oxidative stress and cell damage with iron availability to control hepcidin expression.

Hepcidin transcriptional activation critically depends on the bone morphogenetic protein (BMP)-SMAD signaling pathway. BMPs are multifunctional members of the transforming growth factor-β (TGF-β) superfamily that activate hepcidin expression *in cell lines* or *ex vivo* (2-5). *In vivo*, BMP2 and BMP6 are the major regulators of the *Hepcidin* gene expression (6-8). BMP2 and BMP6 are produced predominantly by liver sinusoidal endothelial cells (LSECs) where they act in a paracrine manner on hepatocytes. There, they bind to BMP type I (ALK2/ALK3) and type II (ACVR2A/BMPR2) receptors to activate the SMAD1/5/8 pathway that controls *Hepcidin* transcription (1).

In addition to dietary iron uptake and recycling of senescent erythrocytes by macrophages, hemolysis represents an important physiological and pathological source of circulating iron. During red blood cells (RBCs) breakdown, large amounts of heme and iron are released into the bloodstream. Under conditions of limited hemolysis, free hemoglobin and heme are rapidly scavenged by plasma proteins such as haptoglobin and hemopexin, respectively (9). However, during excessive hemolysis, caused by infection, inflammation, or in the context of genetic disorders such as sickle cell disease (SCD), these buffering systems are overwhelmed, leading to increased levels of unbound heme and iron (9, 10). Free heme acts as a potent damage-associated molecular pattern (DAMP), triggering toll-like receptor 4 (TLR4) signaling and oxidative stress responses (11, 12).

LSECs are specialized endothelial cells separating the blood stream and hepatic parenchyma, and are therefore among the first cells in the liver to encounter inflammatory cues, DAMPs and PAMPs (13). This setting makes them not only crucial sensors of systemic iron levels but also key responders to hemolytic and inflammatory stress. LSECs actively participate in the

clearance of spleen-derived hemolytic products, such as hemoglobin and erythrocytic membrane (14). Moreover, in SCD LSECs scavenge hemoglobin, and their impairment by intracellular accumulation of sickling hemoglobin aggravates liver injury in SCD mice (15). Moreover, in the context of liver disease, such as non-alcoholic steatohepatitis (NASH), LSECs acquire a proinflammatory phenotype and release cytokines and chemokines to recruit immune cells, thus exacerbating inflammation (13). Understanding how LSECs integrate these signals to control *Bmp6* mRNA expression is essential for linking iron metabolism to immune and stress pathways in the liver.

How *Bmp2* and *Bmp6* mRNA expression in LSECs is controlled by iron remains under discussion. Some studies proposed that *Bmp6* upregulation in LSECs requires intracellular iron accumulation, e.g. from uptake of non-transferrin-bound iron (NTBI). NTBI accumulation and the resulting oxidative stress activate nuclear factor erythroid 2-related factor 2 (NRF2) (16, 17) and c-JUN (18), which then induce *Bmp6* transcription in a cell-autonomous manner. Alternatively, iron-mediated *Bmp6* induction in primary cultured LSECs was shown to occur in an NRF2-independent manner via the transcription factor ETS1, which signals downstream of the p38/JNK mitogen-activated protein kinase (MAPK) pathway (19). Moreover, it has been recently demonstrated that target of rapamycin complex 2 (mTORC2) acts as an iron sensor in LSECs. Mechanistically, iron mediates mTORC2 degradation, leading to forkhead box protein O1 (FOXO1)-dependent *Bmp6* upregulation (20).

The model that intracellular iron accumulation by LSECs triggers increased *Bmp6* mRNA levels was challenged by findings in mouse models of hemochromatosis (HC). For example, LSECs from *Hjv*-KO and Fpn(C326S) mice show elevated *Bmp6* mRNA expression despite a cellular molecular signature of iron deficiency (21, 22). Moreover, *Bmp6* mRNA levels increase during aging, despite an unchanged iron content in non-parenchymal cells, while iron deposition is rather localized in hepatocytes (19). Importantly, iron uptake into LSECs via transferrin receptor 1 (TFR1) or the NTBI transporter ZIP8 does not appear to be essential for controlling BMP2 and BMP6 *in vivo*, as the conditional deletion of either in LSECs does not significantly affect systemic iron homeostasis (16, 23, 24). Similarly, the LSEC-specific deletion of the abundantly expressed HC protein HFE leaves iron homeostasis unaffected (25). By contrast, LSEC-specific *Fpn*-KO mice increase *Bmp6* mRNA levels (26). Thus, the iron-sensing process may involve additional liver cell types.

Our previous work provided evidence that the iron-dependent *Bmp6* control in LSECs is driven by a paracrine signaling mechanism, in which hepatocyte-derived factors enhance iron-dependent *Bmp6* induction (22). However, the identity of the signaling pathways and

mediators involved in this cross-talk remained unclear.

Here we identify the MAPK signaling pathway as a regulatory hub that controls *Bmp6* mRNA expression not only to iron-related signals but also to oxidative stress (H_2O_2) and inflammatory stimuli (heme or LPS). With the exception to iron, these signals trigger TLR4 activation and induce different branches of the MAPK pathway. Collectively, our results highlight both shared and stimulus-specific pathways involved in *Bmp6* control and reveal a novel connection between innate immune sensing, oxidative stress and hepatic iron homeostasis. Additionally, we show that hepatocyte-secreted factors modulate the responsiveness of LSECs to all external signals tested, further highlighting the importance of intrahepatic cell-to-cell communication in iron regulation.

Methods

Mice

C57BL/6N wild-type mice and Hbb^{d3th} mice (on a mixed C57BL/6J and DBA/2J genetic background) were housed under specific pathogen-free (SPF) conditions at the Interfakultäre Biomedizinische Forschungseinrichtung (IBF) animal facility, Heidelberg University (Germany). All mice were kept on a standard 12-hour light/dark cycle and fed a standard rodent diet containing 200 ppm iron, with ad libitum access to food (LASQCdiet® Rod18-A, LASvendi, Soest, Germany) and water. All animal breeding and experimental procedures were conducted following institutional and governmental regulations and were approved by the Regierungspräsidium Karlsruhe (T-47/22, T-52/23, T-48/24, T-10/24, G-87/21).

Isolation and culture of primary LSECs and hepatocytes

Primary mouse LSECs and hepatocytes were isolated as previously described with minor modifications (27). Details about primary cell isolation and cell culture treatments are described in the supplementary methods section.

Protein extraction and Western blotting analysis

Protein extraction was performed as described in the supplementary section. Equal amounts of protein were separated by 10% SDS-PAGE and subsequently transferred for Western blotting using the antibodies listed in Table S1. Chemiluminescence signals were captured and quantified using the Vilber Lourmat Fusion-FX imaging system.

Quantitative Real-Time PCR (RT-qPCR)

Total RNA was extracted from cells using RNA-Mini Kits (Bio&Sell # BS67.311.0250) according

to the manufacturer's instructions, and from snap-frozen mouse tissues using TRIzol reagent (Life Technologies #15596018). RNA was reverse-transcribed using random hexamer primers and the RevertAid H Minus Reverse Transcriptase (Life Technologies #EP0452). RT-qPCR was performed using SYBR Green on a StepOnePlus Real-Time PCR System (Applied Biosystems) with the primers listed in Table S2. Results were calculated using the Pfaffl method (28).

RNA sequencing (RNA-seq)

Strand-specific RNA-seq libraries were prepared using the The NEBNext UltraExpress RNA Library Prep Kit and sequenced in single-end mode on a platform of Element AVITI (150 cycles Kit). Details of the RNA-seq data analysis are reported in the supplementary information. RNA-seqdata are available in Biostudies (Arrayexpress) under the accession number E-MTAB-1637.

Statistics analysis

Data are presented as mean ± standard deviation (SD). Statistical analyses were performed using GraphPad Prism version 8. Two-tailed Student's t-tests, one-way ANOVA, or two-way ANOVA were used where appropriate. Statistical significance was defined as $p < 0.05$ (*), $p < 0.01$ (**), $p < 0.001$ (***), and $p < 0.0001$ (****).

Results

The TLR4/MAPK regulatory axis controls *Bmp6* mRNA expression in primary LSECs in presence of hepatocyte secretome

TLRs orchestrate immune responses and cellular activation by detecting PAMPs and DAMPs. LSECs express multiple TLRs, enabling them to sense microbial components and endogenous damage signals. Combined with their efficient scavenger function, this makes LSECs sensitive sentinel cells that initiate acute-phase responses in the liver (13). To investigate whether the activation of TLRs in LSECs can control iron homeostasis via *Bmp6*, we first tested LPS, a membrane component of gram-negative bacteria, as trigger of the innate immune response with reported functions as TLR4 ligand in LSECs (29). Based on our previous findings showing that *Bmp6* mRNA upregulation by iron is enhanced in presence of hepatocyte conditioned medium (CM) in primary cultured LSECs (22), we evaluated the effect of LPS in presence or absence of CM. In addition, we tested the TLR4 ligand heme, a DAMP released during hemolytic processes, such as SCD or sepsis (11, 12). Both LPS and heme

required CM to activate *Bmp6* mRNA expression (Figure 1A). Differently from *Bmp6*, *Bmp2* mRNA levels were not increased by LPS and heme, but rather were reduced in LSECs both, in the presence and absence of hepatocyte CM (Figure S1A).

To assess whether the activation of other TLRs induces *Bmp6* mRNA expression in presence of CM, we treated LSECs with different ligands activating TLR1 to TLR9. Among the tested ligands, the TLR4 agonist LPS strongly increased *Bmp6* mRNA levels, while fibroblast-stimulating lipopeptide-1 (FSL1), which binds TLR2/6, induced a more modest response (Figure 1B). Of note, TLR4 is the most abundantly expressed TLR in primary cultured LSECs (Figure S1B).

We next characterized the *Bmp6* mRNA response to TLR4 activation in more detail. We show that LPS induced *Bmp6* mRNA expression as early as 2 hours after treatment, even at the very low concentration of 0.05 ng/mL (Figure 1C, 1D). Likewise, heme, but not protoporphyrin IX (PPIX), induced *Bmp6* mRNA expression in a time- and dose-dependent manner, indicating that the iron-containing core of heme is essential for this response (Figure 1E, 1F and 1G). Similarly, LSECs treated with 50 µM myoglobin (30), a damage signal detectable in the plasma of patients with heart diseases (31), also increased *Bmp6* mRNA levels in presence of CM (Figure S1C). These data suggest that DAMPs released from other organs, such as the heart, can elicit responses in LSECs that may contribute to the control of systemic iron homeostasis. Whether this mechanism contributes to the iron deficiency reported in a substantial proportion of patients with heart failure remains to be established (32).

To confirm the role of TLR4 in the LPS, heme and myoglobin-controlled *Bmp6* response, we pre-treated LSECs with the TLR4 inhibitor TAK242. TAK242 effectively reduced *Il6* mRNA induction in response to all treatments (Figure S1D-F) and attenuated *Bmp6* mRNA activation by all stimuli (Figure 1H, S1G). This result further supports the importance of TLR4 in the stimulus-mediated *Bmp6* response, while it also implicates contributions by other signaling networks. Importantly, the requirement for hepatocyte-derived factors for the *Bmp6* response to heme and LPS cannot be attributed to increased *Tlr4* mRNA expression, that was rather reduced in LSECs cultured with hepatocyte CM (Figure S1H).

To identify signaling networks involved in *Bmp6* induction following TLR4 activation, we performed transcription factor activity inference analysis on RNA-seq data from primary LSECs treated with or without heme, in presence of hepatocyte CM. Consistent with a function as TLR ligand in LSECs, in gene set enrichment analysis (GSEA), heme exposure showed enriched pathways related to inflammatory signaling (Figure S1I), including increased mRNA expression of pro-inflammatory cytokines (e.g. *Il6, Tnfa, Il1b*, *Il12b*) and chemokines (e.g.,

Cxcl10, *Ccl2*, *Ccl4*) (Figure S1J). In addition, increased activities of key inflammation-related transcription factors (NFkB1 and RELA) were observed (Fig. 1I). Similarly, proinflammatory cytokines were induced upon LPS treatment (Fig. S1K).

To exclude that *Bmp6* upregulation in response to TLR activation is secondary to the synthesis of cytokines or other effectors, we pre-treated LSECs with cycloheximide to inhibit protein synthesis, followed by LPS addition. Our data show that cycloheximide fails to reduce LPS-mediated *Bmp6* induction (Figure 1J), indicating that *Bmp6* is a primary response gene. By contrast, cycloheximide effectively suppressed LPS-induced nitric oxide synthase 2 (*Nos2*) mRNA expression, which requires *de novo* protein synthesis (33), thereby confirming its inhibitory activity (Figure S2A).

Consistent with previous observations that hemolysis impairs endothelial function (10, 12, 15), LSEC exposure to heme reduced the activity of transcription factors maintaining LSEC identity (ETV2 and NOTCH1) (Figure 1I) (34, 35). In addition, the mRNA expression of hallmark LSEC genes, including *Stab2*, *Cd146* (*Mcam*), *Vegfr3* (*Flt4*), *Vegfr2* (*Kdr*), *Oit3*, and *Cd32b* (*Fcgr2b*), was markedly reduced (Figure S2B).

The most upregulated pathway upon heme treatment was the oxidative stress response (Figure S1I). Indeed, the activity of the transcription factor NRF2 (Figure 1I) and mRNA expression of its target genes, including *Hmox1* and *Nqo1*, were strongly increased (Figure S2C). By contrast, myoglobin treatment did not affect *Hmox1* mRNA levels (Figure S2D) and LPS treatment even reduced *Hmox1* and *Nqo1* mRNA expression (Figure S2E), indicating that, unlike heme, LPS did not activate (but possibly suppressed) the NRF2 pathway. Because different TLR4 ligands induce variable responses of NRF2 target genes, while all of them induced *Bmp6*, we conclude that NRF2 is not a common regulatory hub to induce *Bmp6* mRNA expression downstream of TLR signaling.

We next focused on transcription factors acting downstream of the MAPK pathway (JUN, JUND, ELK1 and FOS) that were strongly activated following heme treatment (Figure 1I). MAPK signaling is activated by cell surface receptors such as TLRs, receptor tyrosine kinases (RTKs) and G protein-coupled receptors (GPCRs) which induce one or several signaling branches, including ERK1/2, JNK and p38 that control key cellular processes such as proliferation, differentiation, survival, and stress responses (36). In line with the transcription factor responses in our RNA-seq data analysis, we detected increased phosphorylation of JNK, ERK1/2, and p38 in LSECs following heme stimulation (Figure 2A), and LPS treatment (Figure 2B). Interestingly, LPS treatment significantly activated ERK1/2 also in the absence of hepatocyte CM. However, ERK1/2 activation appeared delayed and was most evident at 4 h

post-treatment. Pre-incubation with hepatocyte-derived factors not only enabled significant JNK and p38 phosphorylation, but also primed LSECs for a more rapid activation by all three MAPK branches in response to LPS, with phosphorylation peaking as early as 1 h post-treatment (Figure S3A). Of note, the treatment of LSECs with hepatocyte CM did not significantly alter MAPK basal activity (Figure S3B). Altogether, these data indicate that hepatocytes secrete factors that alter the magnitude and dynamics of the MAPK pathway activation in LSECs in a stimulus-specific manner.

To next assess whether an activated MAPK signaling pathway controls *Bmp6* induction in LSECs, we treated primary LSECs with pharmacological inhibitors of MAPK components: U0126 (ERK1/2 via MEK1/2), SP600125 (JNK) and SB202190 (p38) (Figure 2C). Pre-treatment of primary LSECs with the JNK inhibitor SP600125 completely blocked LPS-induced *Bmp6* mRNA expression (Figure 2D). Notably, SP600125 not only inhibited JNK activation, but also suppressed LPS-induced phosphorylation of ERK1/2 and p38 (Figure 2E), suggesting off-target effects that may explain its impact on *Bmp6* mRNA expression. Interestingly, U0126 and SB202190 both reduced ERK1/2 and p38 phosphorylation, indicating low specificity towards their target kinases. However, since SP600125 was the only inhibitor effectively decreasing p-JNK levels and abrogating *Bmp6* mRNA induction by LPS, we assume that JNK activity is required for LPS-driven *Bmp6* upregulation (Figure 2D-E).

By contrast, U0126 and SP600125 effectively blocked heme-induced phosphorylation of ERK1/2 and JNK, respectively, while SB202190 had no significant effect (Figure 2F). Inhibition of ERK1/2 and JNK, but not p38, significantly reduced *Bmp6* and *Nqo1* mRNA expression following heme treatment (Figure 2G and Figure S4A), suggesting that MAPK signaling is critical for both *Bmp6* induction and NRF2 pathway activation. However, the inability of SB202190 to effectively reduce p-p38 levels precluded the assessment of the contribution of p38 signaling to heme-induced *Bmp6* expression.

To further explore the contribution of oxidative stress to *Bmp6* induction by heme and LPS, we pre-treated LSECs with the ROS scavenger N-acetyl-L-cysteine (NAC). NAC did not prevent *Bmp6* induction by LPS or heme, suggesting that the mechanism driving *Bmp6* upregulation by these stimuli is not dependent on oxidative stress (Figure S4B).

To obtain *in vivo* evidence supporting heme-driven *Bmp6* induction in LSECs, we next assessed *Bmp6* mRNA levels in the liver of β-thalassemia mice. These mice show increased serum heme and liver *Bmp6* mRNA levels compared with wild-type controls. However, an increased liver iron content may confound the result of *Bmp6* induction by heme (Figure S4C-E).

By contrast, NRF2-target genes were downregulated upon LPS treatment, suggesting that NRF2 is not involved in LPS-driven *Bmp6* regulation. Previous work has shown that MAPK pathway activation is compatible with both suppression and activation of NRF2 in a context- and stimulus-specific manner (37, 38).

Taken together, our results demonstrate that TLR4 activation induces *Bmp6* mRNA expression in LSECs via MAPK signaling, a mechanism shared by both PAMPs (LPS) and DAMPs (heme). Interestingly, the MAPK signaling branches involved in *Bmp6* activation are signal-specific. We show that JNK, alone or in combination with other MAPK branches, is likely responsible for the *Bmp6* response to LPS, whereas both JNK and ERK1/2 contribute to heme-induced *Bmp6* expression.

Iron-induced *Bmp6* mRNA expression requires the activation of MAPK signaling pathway in LSECs

We next tested whether the MAPK pathway is further required for activating *Bmp6* mRNA expression in primary LSEC cultures maintained with hepatocyte CM with and without iron, as previously established (22). Our data showed that iron treatment of primary LSECs increased the levels of phosphorylated ERK1/2 in a time-dependent manner (Figure 3A). This finding is consistent with the fact that FeNTA induces ROS accumulation, which can activate ERK1/2 (39). Other branches of the MAPK pathway remained unaffected (JNK) or showed decreased phosphorylation (p38) (Figure 3A). Pharmacological inhibition of the ERK1/2-MAPK pathway targeting RAF (Raf265), MEK1/2 (U0126) and ERK1/2 (Ulixertinib) reduced ERK1/2 phosphorylation, with the exception of Ulixertinib, which blocks the downstream activity of ERK1/2 without affecting its phosphorylation, as previously reported (40) (Figure 3B). All three inhibitors downregulated the MAPK target gene *Ccnd1* (Figure S5A) and, importantly, reduced iron-induced *Bmp6* mRNA expression (Figure 3C), supporting a critical role for the ERK1/2 pathway in controlling *Bmp6* mRNA levels in response to iron in presence of hepatocyte CM. MAPK inhibition also abolished the iron-induced transcription of the NRF2 target genes *Hmox1* and *Nqo1* (Figure S5B), suggesting that MAPK signaling contributes to the regulation of *Bmp6* and well-known NRF2 targets in LSECs.

Oxidative stress induced by H_2O_2 controls *Bmp6* mRNA expression in LSECs via MAPK signaling in presence of hepatocyte CM.

Given that iron is a potent inducer of oxidative stress, we next assessed ROS production in LSECs by iron compared to H_2O_2 treatment. We show that FeNTA treatment generated a stronger and longer-lasting ROS signal than H_2O_2-induced oxidative stress (Figure 4A), as

explained by the short lifetime of H_2O_2 in the cytosol (41). Interestingly, also H_2O_2 treatment increased *Bmp6* mRNA expression only in the presence of hepatocyte CM, while it decreased *Bmp2* mRNA levels, similarly to heme and LPS (Figure 4B, S6A). ROS accumulation and *Bmp6* mRNA induction in response to H_2O_2 were effectively prevented by the ROS scavenger NAC (Figure 4A, C). H_2O_2 also increased the mRNA levels of the NRF2 target genes *Hmox1* and *Nqo1*, although to a lesser extent than FeNTA at 6 h, a response prevented by NAC treatment (Figure S6B). While NAC completely abolished the *Bmp6* response to H_2O_2, it only partially reduced iron-induced *Bmp6*, *Hmox1* and *Nqo1* mRNA expression (Figure 4C, S6B). Notably, NAC treatment was not able to fully restore ROS basal levels in FeNTA-treated LSECs. We therefore cannot exclude the involvement of oxidative stress-dependent mechanisms in controlling FeNTA-mediated *Bmp6* response.

Interestingly, H_2O_2 strongly activated the MAPK signaling pathway, as shown by increased phosphorylation of JNK, ERK1/2 and p38, an effect abolished by NAC (Figure 4D). To assess the role of MAPK signaling in H_2O_2-induced *Bmp6* mRNA expression, we used inhibitors targeting ERK1/2 (U0126), JNK (SP600125) and p38 (SB202190). We show that inhibition of the MAPK pathways abolishes H_2O_2-induced *Bmp6* expression (Figure 4E), suggesting that the oxidative stress-induced *Bmp6* response depends on MAPK activation. Consistently, H_2O_2-induced mRNA expression of *Hmox1* and *Nqo1* was also attenuated by MAPK inhibitors (Figure S6C).

Taken together, these findings demonstrate a critical role of the MAPK signaling pathway in controlling *Bmp6* expression in response to oxidative stress in LSECs.

Discussion

Hepcidin is the master regulator of systemic iron fluxes. It inhibits dietary iron absorption and iron release from stores by binding to FPN expressed on duodenal enterocytes, macrophages and hepatocytes, respectively. Activation of hepcidin expression in hepatocytes by excess iron in the plasma and liver acts in a regulatory negative feedback loop to reduce iron absorption. Hepcidin transcription can be activated in hepatocytes by iron-bound transferrin involving iron sensing mechanisms mediated by the HC-associated proteins HFE, TFR2 and HJV, that directly or indirectly interact with the BMP receptors located on the surface of hepatocytes (1). In addition, hepcidin is an acute-phase protein whose transcription in hepatocytes is activated e.g. via IL-6 and the JAK-STAT signaling pathway (42), or by PAMPs via TLR2 and 6 (43). Interestingly, the hepatocyte-intrinsic mechanisms controlling hepcidin activation in response

to iron, inflammation, hormonal, metabolic or oxidative stress signals are attenuated without active BMP/SMAD signaling (44-46), the major pathway controlling hepcidin gene expression (1). The critical role of an active BMP/SMAD signaling pathway for hepcidin induction has been demonstrated in mice with deficiencies for the HC proteins HJV (47) and HFE (48), as well as for ALK3 (49) and SMAD4 (50), and in cell-based assays testing deletions of the BMP-response element in transfected hepcidin promoter constructs (44). The BMPs required for BMP/SMAD signaling in hepatocytes are produced by LSECs, with BMP6 playing a major role (8). However, a residual hepcidin induction upon LPS treatment is retained in *Bmp6*- and *Hjv*-KO mice and in *Bmp6/Hjv*-double KO mice (51). The same occurs in the case of *Hfe*- and *Hjv*-single and double KO (47).

In this work we uncover that, in addition to iron-related signals, LSECs sense cell damage, redox and immune cues to activate *Bmp6* transcription via the MAPK signaling cascade. It is remarkable that similar signals not only control *Bmp6* in LSECs but also hepcidin in hepatocytes. This points towards an intensive cross-talk between the two cell types, which assures BMP/SMAD pathway activation in hepatocytes once hepcidin-activating external cues have been encountered. Signals controlling *Bmp6* expression in LSECs may thus determine the quantitative response of hepcidin by activating the BMP/SMAD signaling pathway in hepatocytes.

The integrative cross-talk between hepatocytes and LSECs is further supported by the observation that the *Bmp6* response to all tested stimuli is enhanced by the hepatocyte CM. The responsible factor(s) (22) has not yet been identified. It thus appears that hepatocyte-secreted factor(s) prime LSECs, enabling them to upregulate *Bmp6* expression in response to various stimuli. However, the specificity of the response to individual stimuli seems to be determined by the intrinsic signaling machinery of LSECs. In addition, hepatocytes have developed hepatocyte-intrinsic mechanisms to respond to iron-related (52), oxidative stress (53) and inflammatory signals (42, 54) that are enhanced by BMP/SMAD signaling (Figure 5).

All immune and stress signals tested here that induce *Bmp6* mRNA expression do so by activating the MAPK signaling pathway in LSECs. While in the presence of hepatocyte CM iron-related signals mainly activate the ERK1/2 branch, H_2O_2-induced oxidative stress and TLR4 stimulation by heme and LPS activate all three signaling branches, including ERK1/2, p38 and JNK. Of note, without CM, p38 is not activated by LPS, reinforcing the role of the secretome. Formally, the MAPK pathway could be activated secondarily by non-canonical BMP signaling (55). However, we deem autocrine BMP signaling mechanisms as unlikely, as cycloheximide treatment did not alter *Bmp6* upregulation in response to LPS. In addition, our

previous work demonstrated that in murine LSEC primary cultures autocrine responses to BMP2 and BMP6 are blocked despite high expression levels of the required receptor complexes (27).

The analysis of gene response patterns to heme treatment suggests that transcription factors downstream of the MAPK signaling (c-JUN, JUND, ELK1 and FOS) may act as mediators of heme-induced *Bmp6* expression. c-JUN, JUND and FOS are members of the AP-1 transcription factor family, which are well known MAPK pathway effectors working in (hetero)dimers. Their possible involvement in *Bmp6* transcription is in agreement with previous publications indicating c-JUN as iron-mediated *Bmp6* regulator (18).

Our findings also extend on previous studies that showed that iron can activate the p38/JNK branch of the MAPK pathway in LSECs, inducing *Bmp6* expression via the transcription factor ETS1 (19). Our data reveal that different branches of the MAPK pathway can mediate the *Bmp6* response. In our experimental setup, *Bmp6* induction by iron is mediated by ERK1/2, while the *Bmp6* response to heme is driven by JNK and ERK1/2. Of note, the effect of p38 on *Bmp6* could not be properly evaluated due to ineffective pharmacological inhibition of the kinase. By contrast, LPS-induced *Bmp6* upregulation is dependent on JNK signaling. Nonetheless, the limited specificity of the JNK inhibitor prevented establishing whether the other MAPK branches are also involved, in combination with JNK, in *Bmp6* modulation by LPS. Differences may be explained by specifics of the model systems and treatment used as well as LSEC isolation and culturing methods. For example, Zurawska et al. showed that 1 mM ferric citrate activates p38 and *Bmp6* mRNA expression (19). By contrast, Fisher et al. reported that 200 µg/mL ferric ammonium citrate requires c-JUN to upregulate *Bmp6*, supporting a role of JNK. However, LSEC-specific *Jun*-KO mice do not show altered *Bmp6* and iron levels (18). Our results were obtained in primary murine LSEC cultures, which contain fenestrae (as observed *in vivo*), and express the LSEC-specific surface marker STAB2 (27).
It is also relevant to consider that the specificity of inhibitors of the various MAPK branches is limited (Figure 2E, F). Although different MAPK branches have been implicated as drivers of *Bmp6* induction, crosstalk frequently occurs among the canonical ERK, JNK, and p38 MAPK pathways (36). MAPK signaling also interacts with the mTORC2–FOXO1 axis, recently identified as an iron-responsive sensor controlling *Bmp6* expression in endothelial cells signaling (20, 56). Although we have not directly addressed the contribution of FOXO1 or mTORC2 to the *Bmp6* response to PAMPs, DAMPs or oxidative stress, transcription factor activity analysis of RNA-seq data from heme-treated LSECs showed significant activation of the FOXO1 transcription factor compared to untreated controls (score 2.76, $p < 0.01$).

While we did not identify a common transcription factor activated downstream of the MAPK

pathway that is responsible for the control of *Bmp6* transcription, we show that several transcription factors activated downstream of the MAPK pathway bind in proximity of the transcription start site of the *Bmp6* coding region, including JUN, FOSL1 and SP1 by interrogating publicly available datasets through the interface ChIP-Atlas (57).

LSECs maintain hepatic immune responses and sustain immune tolerance by monitoring blood arriving from the portal vein that is continuously exposed to gut-derived antigens. LSECs express a wide array of TLRs that respond to a spectrum of ligands, triggering the production of pro-inflammatory cytokines, including TNF-α, IL-6, IL-1β, and IFN-β (13), which is also confirmed by our study (Figure S1J, S1K). We expect that pro-inflammatory cytokines, such as IL-6, together with BMP6, are secreted under inflammatory conditions by LSECs. Such cytokines may act synergistically to enhance hepcidin expression in hepatocytes, explaining why the BMP/SMAD signaling pathway and BMP-RE in the hepcidin promoter are required for the inflammatory activation of hepcidin.

Our findings may be relevant for mechanisms inducing hypoferremia and anemia of inflammation (AI), a widespread disorder caused by chronic inflammatory conditions (58). AI is hallmarked by persistent hepcidin induction in stress conditions, such as infection, iron overload, oxidative stress and hemolysis. Here we show that PAMPs and DAMPs binding to TLR4 in LSECs upregulate *Bmp6*, an essential activator of hepcidin, suggesting that this mechanism may contribute to the generation of hypoferremia and AI.

The role of TLRs in activating *Bmp6* via MAPK signaling illuminates previous findings describing how TLRs expressed in macrophages recognize PAMPs and DAMPs and induce the production of inflammatory mediators (e.g. IL-6) that upregulate hepcidin in hepatocytes. More recently, TLR2/6 sensing in hepatocytes was further shown to directly induce *Hepcidin* mRNA expression via the MAPK signaling pathway (43). Taken together, these data suggest that PAMPs and DAMPs are sensed by several liver cell types via TLRs to control hepcidin and systemic iron homeostasis in a concerted manner. Future experiments are needed to validate our findings *in vivo*.

There are limitations to our study. One is the lack of genetic validations of our findings, which predominantly rely on the use of pharmacological inhibitors. In addition, the MAPK pathway inhibitors applied also affect the expression of NRF2 target genes, thus making it impossible to independently assess contributions of the two pathways to *Bmp6* expression control in response to iron, heme, and H_2O_2. Moreover, future *in vivo* studies are required to validate the involvement of TLR4 and the MAPK pathway components for the *Bmp6* response of LSECs to DAMPs and PAMPs. In addition, it will be of interest to study the contribution of the LSEC-

derived *Bmp6* induction in response to DAMPs and PAMPs on hepcidin production in hepatocytes.

Taken together, our data fill an important knowledge gap by establishing LSECs as essential regulators of iron homeostasis during hemolysis, infection, and exposure to endogenous damage signals connecting innate immune sensing to the control of systemic iron homeostasis.

References

1. Galy B, Conrad M, Muckenthaler M. Mechanisms controlling cellular and systemic iron homeostasis. Nat Rev Mol Cell Biol. 2024;25(2):133-155.

2. Xia Y, Babitt JL, Sidis Y, Chung RT, Lin HY. Hemojuvelin regulates hepcidin expression via a selective subset of BMP ligands and receptors independently of neogenin. Blood. 2008;111(10):5195-204.

3. Truksa J, Peng H, Lee P, Beutler E. Bone morphogenetic proteins 2, 4, and 9 stimulate murine hepcidin 1 expression independently of Hfe, transferrin receptor 2 (Tfr2), and IL-6. Proc Natl Acad Sci U S A. 2006;103(27):10289-10293.

4. Pauk M, Grgurevic L, Brkljacic J, et al. Exogenous BMP7 corrects plasma iron overload and bone loss in Bmp6-/- mice. Int Orthop. 2015;39(1):161-172.

5. Xiao X, Xu Y, Moschetta GA, Yu Y, Fisher AL, Alfaro-Magallanes VM. BMP5 contributes to hepcidin regulation and systemic iron homeostasis in mice. Blood. 2023;142(15):1312-1322.

6. Andriopoulos B Jr, Corradini E, Xia Y, et al. BMP6 is a key endogenous regulator of hepcidin expression and iron metabolism. Nat Genet. 2009;41(4):482-487.

7. Koch PS, Olsavszky V, Ulbrich F, et al. Angiocrine Bmp2 signaling in murine liver controls normal iron homeostasis. Blood. 2017;129(4):415-419.

8. Canali S, Zumbrennen-Bullough KB, Core AB, et al. Endothelial cells produce bone morphogenetic protein 6 required for iron homeostasis in mice. Blood. 2017;129(4):405-414.

9. Duarte TL, Viveiros N, Godinho C, Duarte D. Heme (dys)homeostasis and liver disease. Front Physiol. 2024;15:1436897.

10. Vinchi F, Sparla R, Passos ST, et al. Vasculo-toxic and pro-inflammatory action of unbound haemoglobin, haem and iron in transfusion-dependent patients with haemolytic anaemias. Br J Haematol. 2021;193(3):637-658.

11. Vinchi F, Costa da Silva M, Ingoglia G, et al. Hemopexin therapy reverts heme-induced proinflammatory phenotypic switching of macrophages in a mouse model of sickle cell disease. Blood. 2016;127(4):473-486.

12. Belcher JD, Chen C, Nguyen J, et al. Heme triggers TLR4 signaling leading to endothelial cell activation and vaso-occlusion in murine sickle cell disease. Blood. 2014;123(3):377-390.

13. Wang X-K, Peng Z-G. Targeting Liver sinusoidal endothelial cells: an attractive therapeutic strategy to control inflammation in nonalcoholic fatty liver disease. Front Pharmacol. 2021;12:655557.

14. Zurawska G, Sas Z, Jończy A, et al. Liver sinusoidal endothelial cells constitute a major route for hemoglobin clearance. EMBO Rep. 2026;27(3):598-628.

15. Kaminski TW, Katoch O, Li Z, et al. Impaired hemoglobin clearance by sinusoidal endothelium promotes vaso-occlusion and liver injury in sickle cell disease. Haematologica. 2024;109(5):1535-1550.

16. Charlebois E, Fillebeen C, Presley J, et al. Liver sinusoidal endothelial cells induce BMP6 expression in response to non-transferrin bound iron. Blood. 2022;141(3):271-284.

17. Lim PJ, Duarte TL, Arezes J, et al. Nrf2 controls iron homoeostasis in haemochromatosis and thalassaemia via Bmp6 and hepcidin. Nat Metab. 2019;1(5):519-531.

18. Fisher AL, Wang CY, Xu Y, et al. Quantitative proteomics and RNA-sequencing of mouse liver endothelial cells identify novel regulators of BMP6 by iron. iScience. 2023;26(12):108555.

19. Zurawska G, Jończy A, Niklewicz M, et al. Iron-triggered signaling via ETS1 and the p38/JNK MAPK pathway regulates Bmp6 expression. Am J Hematol. 2024;99(4):543-554.

20. Zhao W, Wang P, Liu Z, et al. The endothelial mTORC2-Foxo1 axis serves as an iron-responsive sensor governing systemic iron homeostasis. Blood. 2025;146(14):1722-1736.

21. Rausa M, Pagani A, Nai A, et al. Bmp6 expression in murine liver non parenchymal cells: a mechanism to control their high iron exporter activity and protect hepatocytes from iron overload? PLoS One. 2015;10(4):e0122696.

22. Colucci S, Altamura S, Marques O, et al. Iron-dependent BMP6 Regulation in liver sinusoidal endothelial cells is instructed by hepatocyte-derived secretory signals. Hemasphere. 2022;6(10):e773.

23. Fisher AL, Wang C-y, Xu Y, et al. Functional role of endothelial transferrin receptor 1 in iron sensing and homeostasis. Am J Hematol. 2022;97(12):1548-1559.

24. Fisher AL, Phillips S, Wang C-Y, et al. Endothelial ZIP8 plays a minor role in BMP6 regulation by iron in mice. Blood. 2024;143(23):2433-2437.

25. Colucci S, Müdder K, Muckenthaler MU, Altamura S. Hfe is highly expressed in liver sinusoidal endothelial cells but is not needed to maintain systemic iron homeostasis in vivo. Hemasphere. 2022;6(1):e667.

26. Fisher AL, Phillips S, Wang CY, et al. The hepcidin-ferroportin axis modulates liver endothelial cell BMP expression to influence iron homeostasis in mice. Blood. 2025;145(6):625-634.

27. Colucci S, Altamura S, Marques O, et al. Liver sinusoidal endothelial cells suppress bone morphogenetic protein 2 production in response to TGFβ pathway activation. Hepatology. 2021;74(4):2186-2200.

28. Pfaffl MW. A new mathematical model for relative quantification in real-time RT-PCR. Nucleic Acids Res.

2001;29(9):e45.

29. Uhrig A, Banafsche R, Kremer M, et al. Development and functional consequences of LPS tolerance in sinusoidal endothelial cells of the liver. J Leukoc Biol. 2005;77(5):626-633.

30. Stone MJ, Waterman MR, Harimoto D, et al. Serum myoglobin level as diagnostic test in patients with acute myocardial infarction. Br Heart J. 1977;39(4):375-380.

31. Kottwitz J, Bruno KA, Berg J, et al. Myoglobin for detection of high-risk patients with acute myocarditis. J Cardiovasc Transl Res. 2020;13(5):853-863.

32. Packer M, Anker SD, Butler J, et al. Redefining iron deficiency in patients with chronic heart failure. Circulation. 2024;150(2):151-161.

33. Weisz A, Oguchi S, Cicatiello L, Esumi H. Dual mechanism for the control of inducible-type NO synthase gene expression in macrophages during activation by interferon-gamma and bacterial lipopolysaccharide. Transcriptional and post-transcriptional regulation. J Biol Chem. 1994;269(11):8324-33.

34. De Smedt J, van Os EA, Talon I, et al. PU.1 drives specification of pluripotent stem cell-derived endothelial cells to LSEC-like cells. Cell Death Dis. 2021;12(1):84.

35. Dill MT, Rothweiler S, Djonov V, et al. Disruption of Notch1 induces vascular remodeling, intussusceptive angiogenesis, and angiosarcomas in livers of mice. Gastroenterology. 2012;142(4):967-977.e2.

36. Plotnikov A, Zehorai E, Procaccia S, Seger R. The MAPK cascades: signaling components, nuclear roles and mechanisms of nuclear translocation. Biochim Biophys Acta. 2011;1813(9):1619-1633.

37. Zipper LM, Mulcahy RT. Erk activation is required for Nrf2 nuclear localization during pyrrolidine dithiocarbamate induction of glutamate cysteine ligase modulatory gene expression in HepG2 cells. Toxicol Sci. 2003;73(1):124-134.

38. Jiang Q, Chen Q, Li C, Gong Z, Li Z, Ding S. ox-LDL-induced endothelial progenitor cell oxidative stress via p38/Keap1/Nrf2 pathway. Stem Cells Int. 2022;2022:5897194.

39. Son Y, Cheong YK, Kim NH, Chung HT, Kang DG, Pae HO. Mitogen-activated protein kinases and reactive oxygen species: how can ROS Activate MAPK pathways? J Signal Transduct. 2011;2011:792639.

40. Qiu R, Alikhanyan K, Volk N, et al. Repression of the iron exporter ferroportin may contribute to hepatocyte iron overload in individuals with type 2 diabetes. Mol Metab. 2022;66:101644.

41. Lim JB, Huang BK, Deen WM, Sikes HD. Analysis of the lifetime and spatial localization of hydrogen peroxide generated in the cytosol using a reduced kinetic model. Free Radic Biol Med. 2015;89:47-53.

42. Verga Falzacappa MV, Vujic Spasic M, Kessler R, Stolte J, Hentze MW, Muckenthaler MU. STAT3 mediates

hepatic hepcidin expression and its inflammatory stimulation. Blood. 2006;109(1):353-358.

43. Bonitz K, Colucci S, Qiu R, et al. Hepatocyte Toll-like receptors contribute to the hepcidin inflammatory response to pathogens and pathogen-derived ligands. Hemasphere. 2025;9(4):e70096.

44. Mleczko-Sanecka K, Roche F, Rita da Silva A, et al. Unbiased RNAi screen for hepcidin regulators links hepcidin suppression to proliferative Ras/RAF and nutrient-dependent mTOR signaling. Blood. 2014;123(10):1574-1585.

45. Verga Falzacappa MV, Casanovas G, Hentze MW, Muckenthaler MU. A bone morphogenetic protein (BMP)-responsive element in the hepcidin promoter controls HFE2-mediated hepatic hepcidin expression and its response to IL-6 in cultured cells. J Mol Med (Berl). 2008;86(5):531-540.

46. Casanovas G, Mleczko-Sanecka K, Altamura S, Hentze MW, Muckenthaler MU. Bone morphogenetic protein (BMP)-responsive elements located in the proximal and distal hepcidin promoter are critical for its response to HJV/BMP/SMAD. J Mol Med (Berl). 2009;87(5):471-480.

47. Fillebeen C, Wilkinson N, Charlebois E, Katsarou A, Wagner J, Pantopoulos K. Hepcidin-mediated hypoferremic response to acute inflammation requires a threshold of Bmp6/Hjv/Smad signaling. Blood. 2018;132(17):1829-1841.

48. Roy CN, Custodio ÁO, de Graaf J, et al. An Hfe-dependent pathway mediates hyposideremia in response to lipopolysaccharide-induced inflammation in mice. Nature Genet. 2004;36(5):481-485.

49. Mayeur C, Lohmeyer LK, Leyton P, et al. The type I BMP receptor Alk3 is required for the induction of hepatic hepcidin gene expression by interleukin-6. Blood. 2014;123(14):2261-2268.

50. Wang R-H, Li C, Xu X, et al. A role of SMAD4 in iron metabolism through the positive regulation of hepcidin expression. Cell Metab. 2005;2(6):399-409.

51. Latour C, Besson-Fournier C, Gourbeyre O, Meynard D, Roth M-P, Coppin H. Deletion of BMP6 worsens the phenotype of HJV-deficient mice and attenuates hepcidin levels reached after LPS challenge. Blood. 2017;130(21):2339-2343.

52. Liu S, Tsyplenkova S, Charlebois E, et al. Tfr2 is necessary for acute iron-dependent hepcidin induction in mice with Tfr1-deficient hepatocytes. Blood. 2026;147(19):2252-2260.

53. Millonig G, Ganzleben I, Peccerella T, et al. Sustained submicromolar H2O2 levels induce hepcidin via signal transducer and activator of transcription 3 (STAT3). J Biol Chem. 2012;287(44):37472-37482.

54. Nemeth E, Rivera S, Gabayan V, et al. IL-6 mediates hypoferremia of inflammation by inducing the synthesis of the iron regulatory hormone hepcidin. J Clin Invest. 2004;113(9):1271-1276.

55. Zhang YE. Non-smad signaling pathways of the TGF-β family. Cold Spring Harb Perspect Biol.

2017;9(2):a022129.

56. Panwar V, Singh A, Bhatt M, et al. Multifaceted role of mTOR (mammalian target of rapamycin) signaling pathway in human health and disease. Signal Transduct Target Ther. 2023;8(1):375.

57. Zou Z, Ohta T, Oki S. ChIP-Atlas 3.0: a data-mining suite to explore chromosome architecture together with large-scale regulome data. Nucleic Acids Res. 2024;52(W1):W45-W53.

58. Marques O, Weiss G, Muckenthaler MU. The role of iron in chronic inflammatory diseases: from mechanisms to treatment options in anemia of inflammation. Blood. 2022;140(19):2011-2023.

Figure legends:

Figure 1. LPS and heme induce *Bmp6* expression in primary LSECs via TLR4.

(A) *Bmp6* mRNA expression in primary LSECs treated with 5 ng/mL LPS or 2.5 μM heme for 6 h in the presence or absence of hepatocyte-conditioned medium. (B) *Bmp6* mRNA expression in primary LSECs treated with various TLR ligands: Pam3CSK4 (TLR1/2), PGN (TLR2), Poly I:C (TLR3), LPS (TLR4), FLA-ST (TLR5), FSL1 (TLR2/6), R848 (TLR7/8), and ODN (TLR9) or vehicle control (NT, non-treated) for 6 h. (C-D) *Bmp6* mRNA expression in primary LSECs treated with increasing concentrations of LPS for 6 h or with 5 ng/mL LPS for 2, 4, and 6 h. (E) *Bmp6* mRNA expression in LSECs treated with 2.5 μM heme or protoporphyrin IX (PPIX) for 6 h. (F-G) *Bmp6* mRNA expression in primary LSECs treated with increasing concentrations of heme for 6 h or treated with 2.5 μM heme for 2, 4, or 6 h. (H) *Bmp6* mRNA expression in primary LSECs pre-treated with TAK242 (5 μM) or DMSO for 1 h, followed by 5 ng/mL LPS or 2.5 μM heme treatment for 6 h. (I) Transcription factor activity analysis by RNA-seq of LSECs treated with heme with respect to untreated controls (contrast-wise), in presence of hepatocyte-conditioned medium. (J) *Bmp6* mRNA expression in primary LSECs pre-treated with CHX (5 μM) or DMSO for 1 h, followed by 5 ng/mL LPS treatment for 6 h. Cell culture experiments, except those in panel A, were always conducted in the presence of hepatocyte-conditioned medium. Gene expression levels were assessed by RT-qPCR, normalized to the housekeeping gene *Rpl19*, and expressed as fold change relative to vehicle-treated controls. The dashed line (ut) represents the mRNA expression of LSECs treated with the conditions shown, in the absence of LPS or heme. Data are obtained from three or four independent experiments and displayed as mean ± SD. Statistical significance: *p<0.05, **p<0.01, ***p<0.001, ****p<0.0001, one-way ANOVA or Student's t-test. CM, conditioned medium; PPIX, protoporphyrin IX; CHX, cycloheximide.

Figure 2. LPS and heme-induced *Bmp6* expression depend on MAPK signaling.

(A-B) Western blot analysis and quantification of phosphorylated and total JNK, ERK1/2, and p38 in LSECs treated with 2.5 μM heme or 5 ng/mL LPS for the indicated time points (15 min to 4 h). (C) Scheme showing the MAPK branches inhibitors and their expected target kinases. (D) *Bmp6* mRNA expression in primary LSECs pre-treated with U0126 (10 μM), SP600125 (5 μM), SB202190 (10 μM), or DMSO for 1 h, followed by 5 ng/mL LPS treatment for 6 h. (E-F) Western blot analysis of phospho-JNK, JNK, phospho-ERK1/2, ERK1/2, phospho-p38, and p38 in primary LSECs pre-treated with U0126 (10 μM), SP600125 (5 μM), SB202190 (10 μM), or DMSO for 1 h, followed by 5 ng/mL LPS or 2.5 μM heme for 1 h. (G) *Bmp6* mRNA expression in primary LSECs pre-treated with the inhibitors described in panel C, followed by

2.5 µM heme treatment for 6 h. All cell culture experiments were conducted in the presence of hepatocyte-conditioned medium. Gene expression levels were assessed by RT-qPCR, normalized to the housekeeping gene *Rpl19*, and expressed as fold change relative to vehicle-treated controls. The dashed line (ut) represents the mRNA expression of LSECs treated with the conditions shown, in the absence of LPS and heme. Data are obtained from three independent experiments and displayed as mean ± SD. Western blots in panels A-B, E-F show a representative replicate of independent experiments. Densitometric quantification displays mean ± SD of three biological replicates. Statistical significance: *p<0.05, **p<0.01, ***p<0.001, ****p<0.0001, one-way ANOVA or Student's t-test.

Figure 3: The MAPK signaling pathway is involved in iron-induced *Bmp6* expression in LSECs in the presence of hepatocyte-conditioned medium.

(A) Western blot analysis and quantification of phospho-JNK, JNK, phospho-ERK1/2, ERK1/2, phospho-p38, and p38 in primary LSECs stimulated with 50 µM FeNTA. (B) Western blot analysis of phospho-ERK1/2 and total ERK1/2 in primary LSECs pre-treated with RAF265, U0126, Ulixertinib, or DMSO as in (C), followed by 50 µM FeNTA for 1 h. (C) *Bmp6* mRNA expression in primary LSECs pre-treated with RAF265 (5 µM), U0126 (10 µM), Ulixertinib (10 µM), or DMSO for 1 h, followed by 50 µM FeNTA for 6 h. All cell culture experiments were conducted in the presence of hepatocyte-conditioned medium. Data in C are RT-qPCR results, normalized to the housekeeping gene *Rpl19* and presented as fold change relative to vehicle controls. The dashed line (ut) indicates the *Bmp6* mRNA expression of LSECs treated with DMSO or the inhibitors in the absence of FeNTA. Data are derived from three independent experiments and presented as mean ± SD. Western blots in panels A-B show a representative replicate of three independent experiments. Densitometric quantification displays mean ± SD of all biological replicates. Statistical significance: *p<0.05, **p<0.01, ***p<0.001, one-way ANOVA or Student's t-test. FeNTA, ferric nitrilotriacetate.

Figure 4: Oxidative stress-induced *Bmp6* expression depends on MAPK signaling pathway in the presence of hepatocyte-conditioned medium

(A) Measurement of ROS content in primary LSECs treated with H_2O_2 (100 µM) or FeNTA (50 µM) for 1 or 6 h in the absence or presence of NAC (5 mM), analyzed by flow cytometry. (B) *Bmp6* mRNA expression in primary LSECs treated with 100 µM H_2O_2 or vehicle control (NT, non-treated) for 6 h in the presence or absence of hepatocyte-conditioned medium. (C) *Bmp6* mRNA expression in primary LSECs pre-treated with NAC (5 mM) for 1 h, followed by H_2O_2 (100 µM) or FeNTA (50 µM) treatment for 6 h. (D) Western blot analysis and quantification of phospho-JNK, JNK, phospho-ERK1/2, ERK1/2, phospho-p38, and p38 in primary LSECs pre-

treated with NAC (5 mM) for 1 h and subsequently treated with H_2O_2 (100 µM) for 1 h. (E) *Bmp6* mRNA expression in primary LSECs pre-treated with U0126 (10 µM), SP600125 (5 µM), SB202190 (10 µM), or DMSO for 1 h, followed by H_2O_2 (100 µM) treatment for 6 h. All cell culture experiments in A, C, D, and E were conducted in the presence of hepatocyte-conditioned medium. Data in (B, C and E) are RT-qPCR results, normalized to *Rpl19* and presented as fold change compared to vehicle controls. The dashed line (ut) represents the mRNA expression of LSECs treated with the conditions shown, in the absence of H_2O_2. Data are obtained from three independent experiments and displayed as mean ± SD. The western blot in panels D shows a representative replicate of three independent experiments. Densitometric quantification displays mean ± SD of all biological replicates. Statistical significance: *p<0.05, **p<0.01, ****p<0.0001, one-way ANOVA, two-way ANOVA or Student's t-test. CM, conditioned medium; FeNTA, ferric nitrilotriacetate; NAC, N-Acetyl-L-Cysteine.

Figure 5: Working model of LSEC *Bmp6* regulation and hepcidin induction by iron, inflammatory and redox signals

In the presence of hepatocyte secreted factors, LSECs integrate iron, inflammatory (heme, myoglobin and LPS) and redox (H_2O_2) signals to induce *Bmp6* mRNA expression via the MAPK signaling pathway. While TLR4 mediates the response to inflammatory stimuli, the iron sensing receptor is still unknown. Most tested stimuli also activate the NRF2-mediated antioxidant response. However, how NRF2 interacts with the MAPK pathway for *Bmp6* regulation remains to be investigated. Upon its release in the space of Disse, BMP6 binds to the BMP receptor complex on the surface of hepatocytes, resulting in the activation of the SMAD signaling pathway. The active SMAD1/5/8-SMAD4 complex then binds to the BMP-responsive element (BMP-RE) in the promoter of the *Hepcidin* gene, allowing its transcription. Previous data have shown that *Hepcidin* induction by inflammatory stimuli via the JAK-STAT pathway requires a functional BMP-RE, in addition to the STAT-RE, in the *Hepcidin* promoter. Similarly, active BMP signaling contributes to the inflammation-mediated *Hepcidin* induction in hepatocytes. Inflammatory cues can also activate hepcidin transcription via the TLRs-MAPK axis. However, a dependency on the BMP pathway has not been studied in this case. LPS, lipopolysaccharide; TLR, Toll-like receptor.

Figure 1

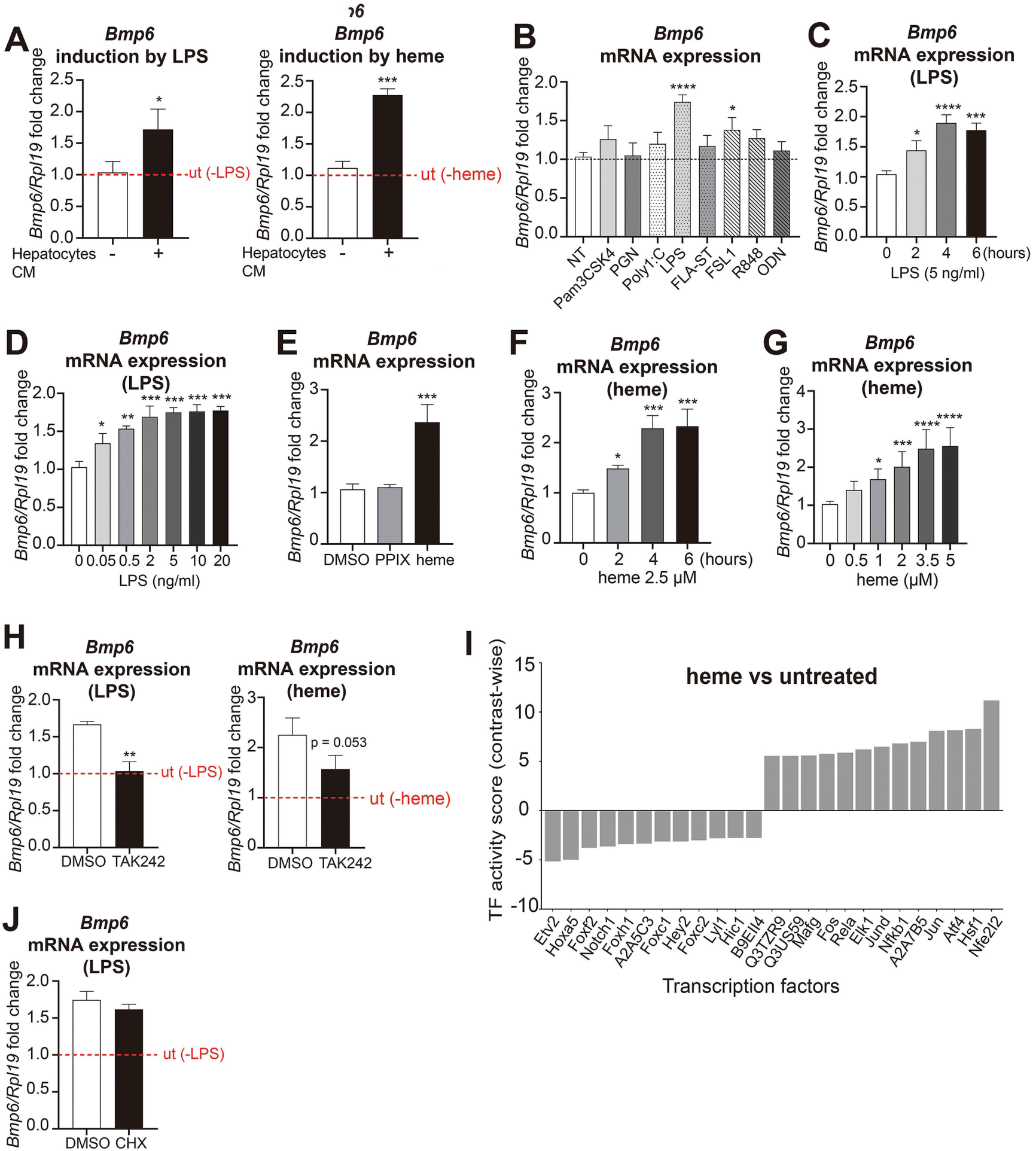
A
Bmp6 induction by LPS
Bmp6/Rpl19 fold change
ut (-LPS)
Hepatocytes
CM
Bmp6 induction by heme
ut (-heme)
B
Bmp6 mRNA expression
NT
Pam3CSK4
PGN
Poly1:C
LPS
FLA-ST
FSL1
R848
ODN
C
Bmp6 mRNA expression (LPS)
LPS (5 ng/ml)
D
Bmp6 mRNA expression (LPS)
LPS (ng/ml)
E
Bmp6 mRNA expression
DMSO
PPIX
heme
F
Bmp6 mRNA expression (heme)
heme 2.5 µM
G
Bmp6 mRNA expression (heme)
heme (µM)
H
Bmp6 mRNA expression (LPS)
DMSO
TAK242
Bmp6 mRNA expression (heme)
p = 0.053
I
heme vs untreated
TF activity score (contrast-wise)
Etv2
Hoxa5
Foxf2
Notch1
Foxh1
A2A5C3
Foxc1
Hey2
Foxc2
Lyl1
Hic1
B9EII4
Q3TZR9
Q3US59
Mafg
Fos
Rela
Elk1
Jund
Nfkb1
A2A7B5
Jun
Atf4
Hsf1
Nfe2l2
Transcription factors
J
Bmp6 mRNA expression (LPS)
DMSO
CHX

Figure 2

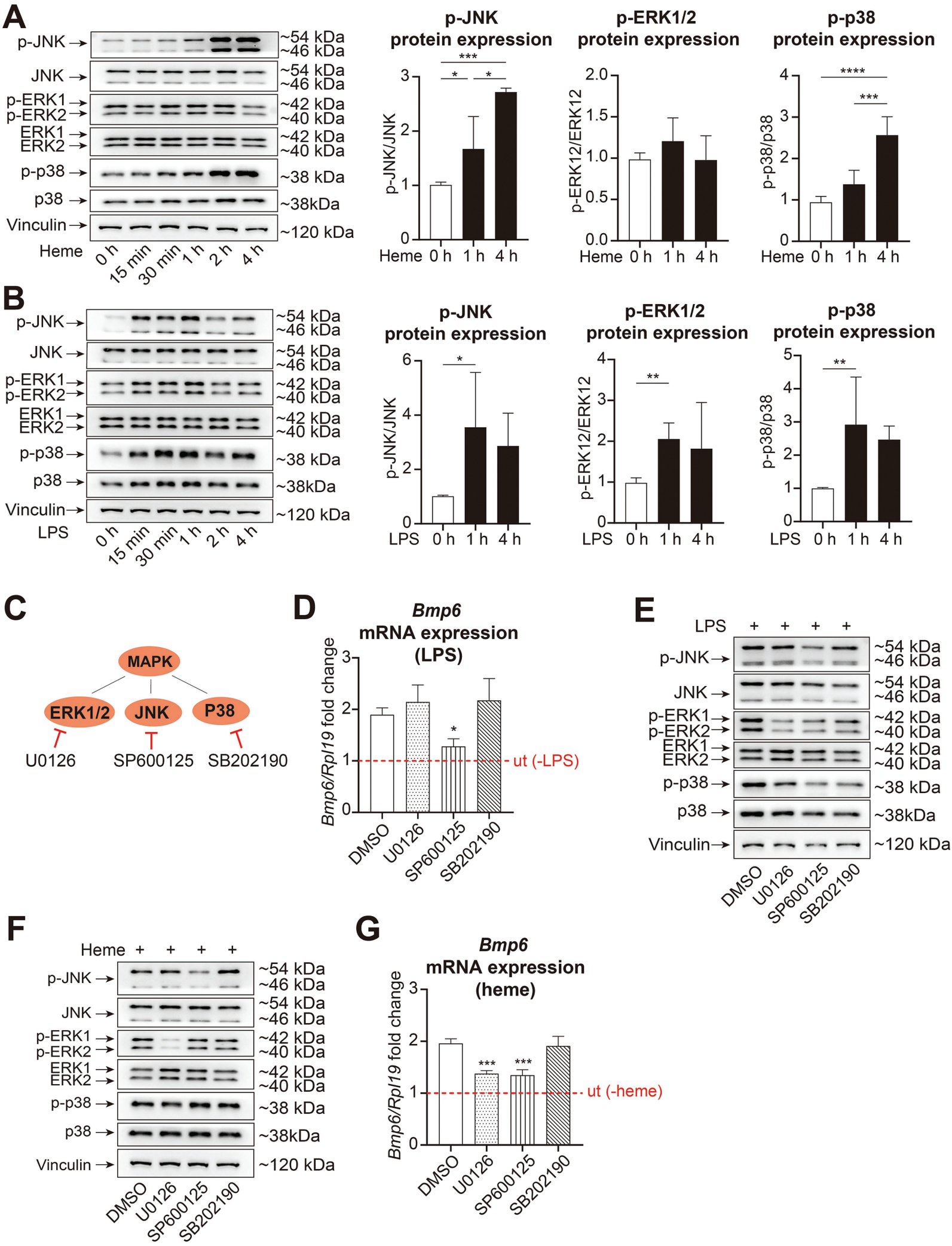
A
p-JNK
JNK
p-ERK1
p-ERK2
ERK1
ERK2
p-p38
p38
Vinculin
~54 kDa
~46 kDa
~42 kDa
~40 kDa
~38 kDa
~38kDa
~120 kDa
Heme
0 h
15 min
30 min
1 h
2 h
4 h
p-JNK protein expression
p-JNK/JNK
p-ERK1/2 protein expression
p-ERK12/ERK12
p-p38 protein expression
p-p38/p38
B
LPS
C
MAPK
ERK1/2
JNK
P38
U0126
SP600125
SB202190
D
Bmp6 mRNA expression (LPS)
Bmp6/Rpl19 fold change
ut (-LPS)
DMSO
E
F
G
Bmp6 mRNA expression (heme)
ut (-heme)

Figure 3

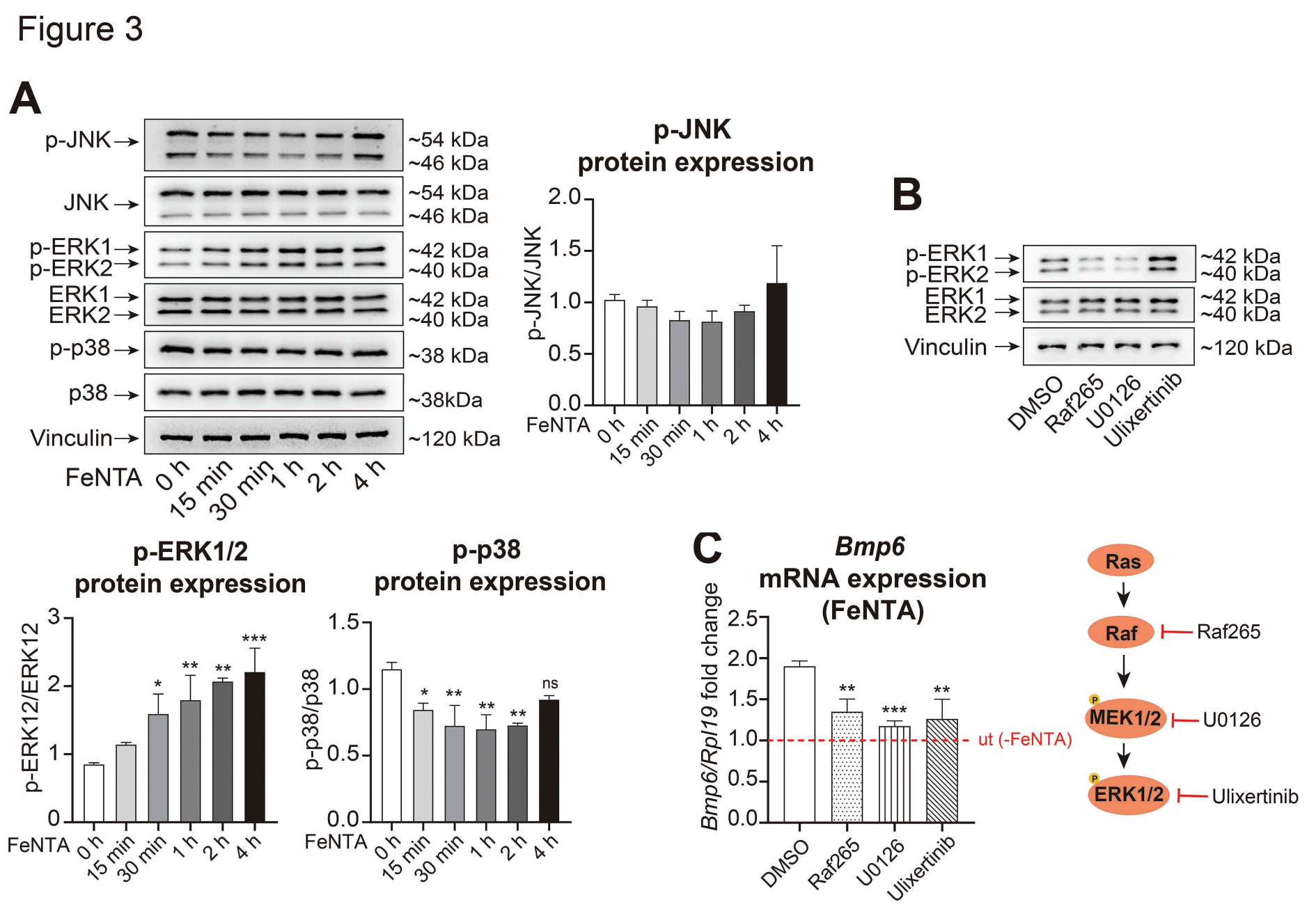
A
p-JNK
JNK
p-ERK1
p-ERK2
ERK1
ERK2
p-p38
p38
Vinculin
~54 kDa
~46 kDa
~42 kDa
~40 kDa
~38 kDa
~38kDa
~120 kDa
FeNTA
0 h
15 min
30 min
1 h
2 h
4 h
p-JNK
protein expression
p-JNK/JNK
B
DMSO
Raf265
U0126
Ulixertinib
p-ERK1/2
protein expression
p-ERK12/ERK12
p-p38
protein expression
p-p38/p38
ns
C
Bmp6
mRNA expression
(FeNTA)
Bmp6/Rpl19 fold change
ut (-FeNTA)
Ras
Raf
MEK1/2
ERK1/2
Raf265
U0126
Ulixertinib

Figure 4

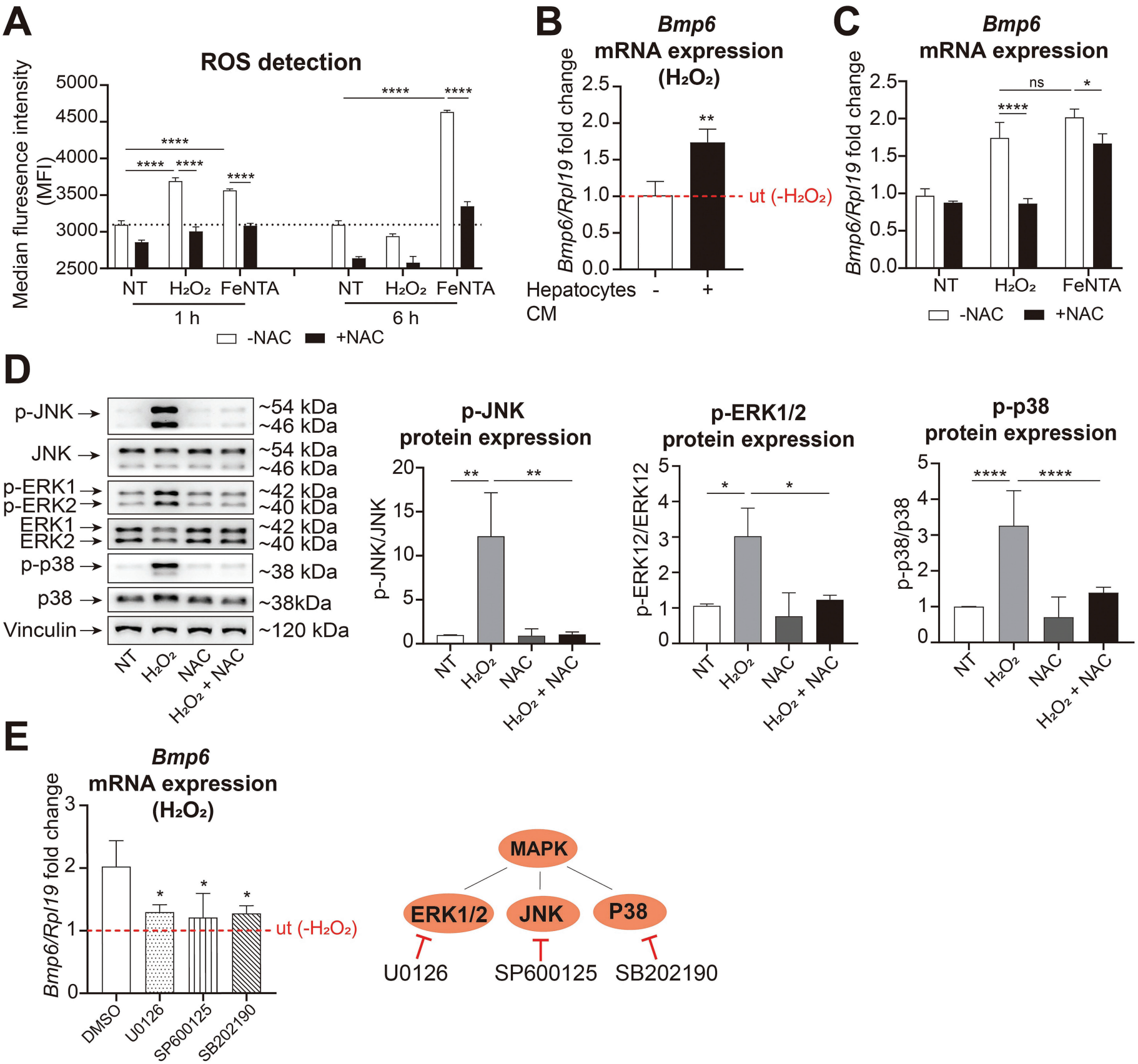
A
ROS detection
Median fluresence intensity (MFI)
5000
4500
4000
3500
3000
2500
****
****
****
****
****
NT
H2O2
FeNTA
NT
H2O2
FeNTA
1 h
6 h
-NAC
+NAC
B
Bmp6
mRNA expression
(H2O2)
Bmp6/Rpl19 fold change
2.5
2.0
1.5
1.0
0.5
0.0
**
ut (-H2O2)
Hepatocytes
CM
-
+
C
Bmp6
mRNA expression
Bmp6/Rpl19 fold change
ns
*
****
NT
H2O2
FeNTA
-NAC
+NAC
D
p-JNK
JNK
p-ERK1
p-ERK2
ERK1
ERK2
p-p38
p38
Vinculin
~54 kDa
~46 kDa
~54 kDa
~46 kDa
~42 kDa
~40 kDa
~42 kDa
~40 kDa
~38 kDa
~38kDa
~120 kDa
NT
H2O2
NAC
H2O2 + NAC
p-JNK
protein expression
p-JNK/JNK
20
15
10
5
0
**
**
p-ERK1/2
protein expression
p-ERK12/ERK12
5
4
3
2
1
0
*
*
p-p38
protein expression
p-p38/p38
5
4
3
2
1
0
****
****
E
Bmp6
mRNA expression
(H2O2)
Bmp6/Rpl19 fold change
3
2
1
0
*
*
*
ut (-H2O2)
DMSO
U0126
SP600125
SB202190
MAPK
ERK1/2
JNK
P38
U0126
SP600125
SB202190

Figure 5

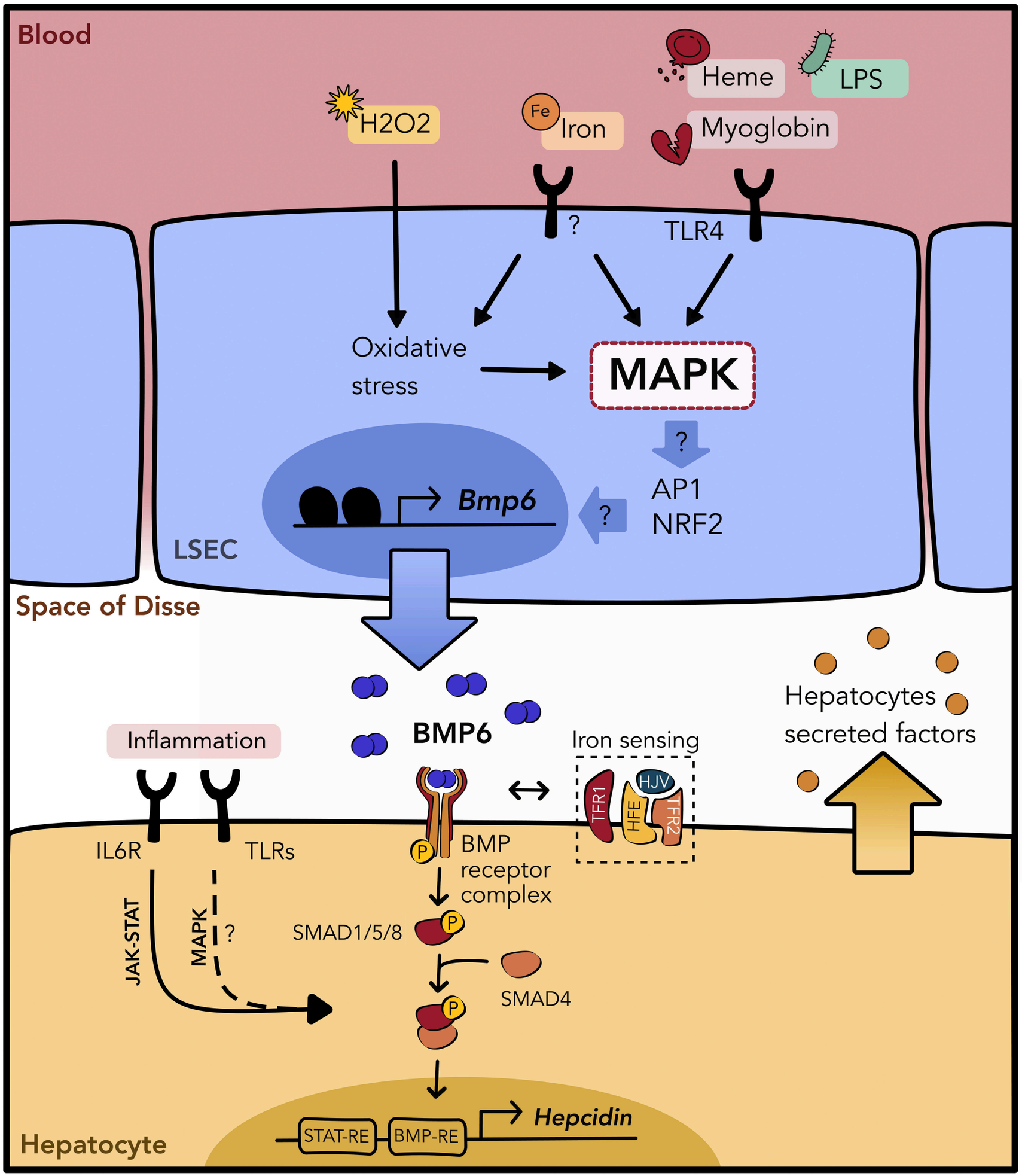
Blood
H2O2
Fe
Iron
Heme
LPS
Myoglobin
?
TLR4
Oxidative stress
MAPK
?
AP1
NRF2
?
Bmp6
LSEC
Space of Disse
BMP6
Inflammation
Iron sensing
Hepatocytes secreted factors
TFR1
HJV
HFE
TFR2
IL6R
TLRs
P
BMP receptor complex
JAK-STAT
MAPK
?
SMAD1/5/8
P
SMAD4
P
Hepcidin
STAT-RE
BMP-RE
Hepatocyte

Liver sinusoidal endothelial cells integrate metabolic and immune signals for MAPK-dependent BMP6 regulation and hepcidin induction

Ruiyue Qiu[1*], Stefania Cucinelli[1,2,3*], Christina Mertens[1,4], Ana Catarina Pêgo[1,2], Silvia Colucci[1,3], Sandro Altamura[1,2], Alireza Saadatmand[4,5], Johannes Backs[4,5], Matthias W. Hentze[2,3#], Martina U. Muckenthaler[1,2,4,6#]

[1]Department of Pediatric Hematology, Oncology and Immunology, University of Heidelberg, Heidelberg, Germany

[2]Molecular Medicine Partnership Unit, University of Heidelberg, Heidelberg, Germany

[3]European Molecular Biology Laboratory, Heidelberg, Germany

[4]DZHK (German Centre for Cardiovascular Research), Partner Site Heidelberg/Mannheim, Germany

[5]Institute of Experimental Cardiology, University of Heidelberg, Heidelberg, Germany

[6]Translational Lung Research Center Heidelberg (TLRC), German Center for Lung Research (DZL), University of Heidelberg, Heidelberg, Germany

*R.Q. and S.Cu. are joint first authors.

#M.W.H. and M.U.M. are joint last authors.
Corresponding author's details: martina.muckenthaler@med.uni-heidelberg.de

Supplementary methods

Isolation and culture of primary LSECs and hepatocytes

Primary mouse LSECs were isolated following a previously published protocol with minor modifications (1). Briefly, livers from C57BL/6N wild-type mice (22–30 weeks old) were perfused via the vena cava using Liver Perfusion Medium (Life Technologies #17701038), followed by enzymatic digestion with Liberase (Roche #5401127001). After mechanical decapsulation, the resulting liver cell suspension was collected in wash medium (Life Technologies #17704024) and sequentially filtered through 100 µm and 70 µm cell strainers. Hepatocytes and non-parenchymal cells (NPCs) were separated by low-speed centrifugation. Primary hepatocytes were seeded on collagen-coated plates at 2.5×10^5 cells/mL. NPCs were further enriched using density gradient centrifugation with Optiprep (Stemcell Technologies #07820). For primary LSEC culture, LSECs and KCs were separated by differential adhesion steps. LSECs were recovered and plated on collagen-coated plates at a density of 2×10^6 cells/mL. All primary cells were cultured in William's E medium (Life Technologies #32551020) supplemented with 4% fetal bovine serum (FBS) and 1% penicillin/streptomycin, under humidified conditions at 37 °C with 5% CO_2. Vascular endothelial growth factor (VEGF, Life Technologies #450-32) was additionally supplemented at the final concentration of 10 ng/mL. Hepatocyte-conditioned medium was prepared as previously described (2) and added to primary mouse LSECs 1 h before stimulation.

Cell culture treatments

Heme was used in the form of hemin and purchased from Frontiers Specialty Chemicals (#H651-9) and diluted in dimethyl sulfoxide (DMSO) according to the manufacturer's instructions to the indicated concentrations. The TLR4 inhibitor TAK242 (#13871), the MAPK pathway inhibitors RAF265 (#16991), U0126 (#70970), SB202190 (#21201) and Ulixertinib (#18298) were purchased from the Cayman Chemical Company and diluted in DMSO. Lipopolysaccharide (LPS) (#2630), myoglobin (#M1882), N-acetyl-L-cysteine (NAC) (#A7250), H_2O_2 (#1.07209) and cycloheximide (CHX) (#01810) were purchased from Sigma-Aldrich/Merck and diluted in phosphate buffered solution (PBS) (LPS, myoglobin, NAC and H_2O_2) or DMSO (CHX). The TLR ligands Pam3CSK4 (TLR2:1) (#tlrl-pms), PGN‐SA (TLR2) (#tlrl-pgns2), Poly I:C (TLR3) (#tlrl-picw), FLA-ST (TLR5) (#tlrl-stfla), FSL1 (TLR2:TLR6) (tlrl-fsl), R848 (TLR7:8) (#tlrl-r848-1), ODN (TLR9) (#tlrl-1826) and the MAPK inhibitor SP600125 (#tlrl-sp60) were purchased form Invivogen and diluted in PBS (TLR ligands) or DMSO (SP600125). Ferric nitrilotriacetate (FeNTA) was prepared dissolving iron (III) chloride hexahydrate (Sigma-Aldrich/Merck #31232) and nitrilotriacetic acid disodium salt (NTA) (Sigma-Aldrich/Merck #N0128) in ratio 1:4 in PBS.

Protein extraction

Total protein lysates were prepared by homogenizing cell pellets in radioimmunoprecipitation assay (RIPA) buffer supplemented with a protease inhibitor cocktail (cOmplete™, Roche #04693116001) and phosphatase inhibitors (PhosSTOP™, Roche #04906845001). Protein concentrations were determined using the bicinchoninic acid (BCA) assay (Life Technologies #23228, #23224). Equal amounts of protein (20 µg per sample) were loaded for SDS-PAGE and Western Blot.

Reactive oxygen species (ROS) measurement

Intracellular ROS levels in LSECs were detected using the CellROX® Green Flow Cytometry Assay Kit (Life Technologies #C10492) according to the manufacturer's instructions. Following treatments, cells were incubated with 500 nM CellROX® Green for 30 minutes, then stained with 5 nM SYTOX® Red Dead Cell Stain (Life Technologies #S34859) for 5 minutes. Fluorescence intensity and the percentage of ROS-positive, live cells were measured using a BD Accuri™ C6 Plus flow cytometer.

Tissue iron quantification

Tissue non-heme iron content was quantified using the Bathophenanthroline method (3) and normalized to the dry weight of the tissue samples.

Serum heme measurement

Serum heme concentrations were determined fluorometrically as previously described (4). Briefly, 5 µL of serum was incubated with 500 µL of 1 M oxalic acid (Sigma-Aldrich #75688) at 99 °C for 30 minutes. Fluorescence emission was measured at an excitation wavelength of 405 nm and an emission wavelength of 660 nm. Background fluorescence was evaluated in non-boiled samples.

RNA sequencing (RNA-seq) data analysis

Reads were aligned to the GRCm39 genome using STAR aligner (2.7.11b) (5). Transcription factor inference analysis was conducted using the CollecTRI (Collection of Transcriptional Regulatory Interactions) resource with the univariate linear model available from the decoupleR (v2.14.0) package (6). Gene Set Enrichment Analysis (GSEA) was performed using the GSEA software 4.4.0 (7). Differential expression analysis has been performed using the R library DESeq2 (v1.48.1) (8) and statistics (*) refers to p-adjusted values.

Supplementary tables

Table S1: List of antibodies and dilutions

Target protein	Dilution ratio	Source	Provider	Catalog No.
Mouse IgG	1:5000	Rabbit	Sigma-Aldrich/Merck	A9044
Rabbit IgG	1:5000	Goat	Sigma-Aldrich/Merck	A0545
AKT	1:1000	Rabbit	Cell Signaling	9272S
ERK1/2	1:1000	Rabbit	Cell Signaling	4695
JNK	1:1000	Rabbit	Cell Signaling	9252
p38 MAPK	1:1000	Rabbit	Cell Signaling	8690
Phospho-AKT (Ser473)	1:1000	Rabbit	Cell Signaling	4060
Phospho-ERK1/2 (Thr202/Tyr204)	1:1000	Rabbit	Cell Signaling	4370
Phospho-JNK (Thr183/Tyr185)	1:1000	Rabbit	Cell Signaling	4668
Phospho-p38 MAPK (Thr180/Tyr182)	1:1000	Rabbit	Cell Signaling	4511
Vinculin	1:1000	Mouse	Sigma-Aldrich/Merck	SAB4503069

Table S2 List of RT-qPCR primers

Target gene	**Forward primer 5'- 3'**	**Reverse primer 5'- 3'**
Bmp2	GCGCAGCTTCCATCACGA	CCCACTCATCTCTGGAAGTTCCT
Bmp6	ATGGCAGGACTGGATCATTGC	CCATCACAGTAGTTGGCAGCG
Ccnd1	GCAGAAGGAGATTGTGCCATCC	AGGAAGCGGTCCAGGTAGTTCA
Hmox1	AGGCTAAGACCGCCTTCCT	TGTGTTCCTCTGTCAGCATCA
Il6	GCTACCAAACTGGATATAATCAGGA	CCAGGTAGCTATGGTACTCCAGAA
Nos2	GAGACAGGGAAGTCTGAAGCAC	CCAGCAGTAGTTGCTCCTCTTC
Nqo1	AGCGTTCGGTATTACGATCC	AGTACAATCAGGGCTCTTCTCG
Rpl19	AGGCATATGGGCATAGGGAAGAG	TTGACCTTCAGGTACAGGCTGTG
Tlr4	GATCTGAGCTTCAACCCCCTG	TCCACAGCCACCAGATTCTC
Tnfα	TGCCTATGTCTCAGCCTCTTC	GAGGCCATTTGGGAACTTCT

Supplementary results

Figure legends:

Figure S1. TLR4 activation by LPS, heme, and myoglobin drives pro-inflammatory cytokine production

(A) *Bmp2* mRNA expression in primary LSECs treated with 5 ng/mL LPS or 2.5 µM heme for 6 h in the presence or absence of hepatocyte-conditioned medium. (B) Expression profile of *Tlr1–9* mRNA in primary cultured LSECs (n = 3). (C) *Bmp6* mRNA expression in primary LSECs treated with myoglobin (50 µM) or vehicle control (ut, untreated) for 6 h. (D-F) *Il6* mRNA expression in LSECs pre-treated with TAK242 (5 µM) for 1 h, followed by LPS (5 ng/mL), heme (2.5 µM), or myoglobin (50 µM) treatment for 6 h. (G) *Bmp6* mRNA expression in LSECs pre-treated with TAK242 (5 µM) for 1 h, followed by myoglobin (50 µM) treatment for 6 h. (H) *Tlr4* mRNA expression in primary LSECs in the presence or absence of hepatocyte-conditioned medium for 7 h. (I) Gene set enrichment analysis (GSEA) was performed using the WikiPathways database to identify biological pathways enriched in heme-treated compared to untreated control LSECs. The dotplot shows significant (FDR < 25%) enriched pathways upon LSECs treatment. The normalized enrichment score (NES) indicates the degree to which a pathway is overrepresented in the heme-treated group. The size of the dots represents the number of genes contributing to each pathway, while the color gradient corresponds to the nominal (NOM) p-value. (J) Heatmap showing significant (adjusted p-value < 0.1) differentially expressed cytokine gene levels in RNA-seq from LSECs treated with heme vs untreated controls. Values are represented as Z-score of log2-transformed expression levels (variance-stabilized transformation from DeSeq2 package) across samples. (K) *Il6* and *Tnfa* mRNA expression in LSECs treated with 5 ng/mL LPS for 6 h. All cell culture experiments in B-G and I-K were conducted in the presence of hepatocyte-conditioned medium. Gene expression levels were assessed by RT-qPCR, normalized to the housekeeping gene *Rpl19*, and expressed as fold change relative to vehicle-treated controls. The dashed line (ut) represents the mRNA expression of LSECs treated with the conditions shown, in the absence of LPS, heme or myoglobin. Data are obtained from three independent experiments and displayed as mean ± SD. Statistical significance: *p<0.05, **p<0.01, ***p<0.001, one-way ANOVA or Student's t-test. CHX, cycloheximide; TPM, transcripts per million; FDR, false discovery rate; LPS, lipopolysaccharide.

Figure S2. LPS, heme and myoglobin differently modulate the expression of NRF2-target genes

(A) *Nos2* mRNA expression in primary LSECs pre-treated with CHX (5 μM) or DMSO for 1 h, followed by 5 ng/mL LPS treatment for 6 h. (B) Heatmap showing significant (adjusted p-value < 0.1) differentially expressed LSEC marker gene levels in RNA-seq from LSECs treated with heme vs untreated controls. Values are represented as Z-score of log2-transformed expression levels (variance-stabilized transformation from DeSeq2 package) across samples. (C) *Hmox1* and *Nqo1* mRNA expression in LSECs treated with 2.5 μM heme for 6 h. (D) *Hmox1* mRNA expression in LSECs treated with myoglobin (50 μM) for 6 h. (E) *Hmox1* and *Nqo1* mRNA expression in LSECs treated with 5 ng/mL LPS. All cell culture experiments were conducted in the presence of hepatocyte-conditioned medium. Gene expression levels were assessed by RT-qPCR, normalized to the housekeeping gene *Rpl19*, and expressed as fold change relative to vehicle-treated controls. The dashed line (ut) in A represents the mRNA expression of LSECs treated with the conditions shown, in the absence of LPS. Data are obtained from three independent experiments and displayed as mean ± SD. Statistical significance: **p<0.01, ***p<0.001, Student's t-test. CHX, cycloheximide; LPS, lipopolysaccharide.

Figure S3. Hepatocyte-derived factors alter the stimulus-specific MAPK pathway activation by LPS.

(A) Western blot analysis and quantification of phosphorylated and total JNK, ERK1/2, and p38 in LSECs treated with 5 ng/mL LPS for the indicated time points in absence of hepatocyte conditioned medium (CM) for the indicated timepoints. (B) Western blot analysis and quantification of phosphorylated and total JNK, ERK1/2, and p38 in LSECs in presence or absence of hepatocytes conditioned medium (CM) for the indicated timepoints. Western blots show a representative replicate of three independent experiments. Densitometric quantification displays mean ± SD of all biological replicates. Statistical significance: *p<0.05, one-way ANOVA. LPS, lipopolysaccharide

Figure S4. *Bmp6* induction by heme or LPS is not dampened by NAC treatment.

(A) *Nqo1* mRNA expression in primary LSECs pre-treated with U0126 (10 μM), SP600125 (5 μM), SB202190 (10 μM), or DMSO for 1 h, followed by 2.5 μM heme treatment for 6 h. (B) *Bmp6* mRNA expression in primary LSECs pre-treated with NAC (5 mM) for 1 h, followed by 2.5 μM heme or 5 ng/mL LPS treatment or vehicle control (NT, non-treated) for 6 h. (C) Liver *Bmp6* mRNA expression in wild-type (WT) or β-thalassemia mice (TH) (females, 11 weeks old). (D) Serum heme or (E) liver iron content of wild-type (WT) or β-thalassemia mice (TH) (females, 11 weeks old). All cell culture experiments were conducted in the presence of hepatocyte-conditioned medium. Gene expression levels were assessed by RT-qPCR,

normalized to the housekeeping gene *Rpl19*, and expressed as fold change relative to vehicle-treated controls. The dashed line (ut) in A represents the mRNA expression of LSECs treated with the conditions shown, in the absence of heme. Data are obtained from three independent experiments and displayed as mean ± SD. Statistical significance: *p<0.05, **p<0.01, ***p<0.001, ****p<0.0001, two-way ANOVA, one-way ANOVA or Student's t-test.

Figure S5. Inhibition of the MAPK signaling pathway decreases FeNTA-induced NRF2 target gene expression.

(A) *Ccnd1* mRNA expression in primary LSECs pre-treated with RAF265 (5 μM), U0126 (10 μM), ulixertinib (10 μM), or DMSO for 6 h. (B) *Hmox1* and *Nqo1* mRNA expression in primary LSECs pre-treated with RAF265 (5 μM), U0126 (10 μM), ulixertinib (10 μM), or DMSO for 1 h, followed by 50 μM FeNTA treatment for 6 h. All experiments were performed in the presence of hepatocyte-conditioned medium. Data are RT-qPCR results, normalized to the housekeeping gene *Rpl19* and presented as fold change relative to vehicle controls. The dashed line (ut) indicates the mRNA expression of LSECs treated with DMSO or the inhibitors in the absence of FeNTA. Data are derived from three independent experiments and presented as mean ± SD. Statistical significance: *p<0.05, **p<0.01, ***p<0.001, ****p<0.0001, one-way ANOVA. FeNTA, ferric nitrilotriacetate.

Figure S6. MAPK signaling is involved in oxidative stress-mediated NRF2 activation.

(A) *Bmp2* mRNA expression in primary LSECs treated with 100 μM H_2O_2 or vehicle control (NT, non-treated) for 6 h in the presence or absence of hepatocyte-conditioned medium. (B) *Hmox1* and *Nqo1* mRNA expression in primary LSECs pre-treated with NAC (5 mM) for 1 h, followed by treatment with H_2O_2 (100 μM), FeNTA (50 μM) or vehicle control (NT, non-treated) for 6 h. (C) *Hmox1* and *Nqo1* mRNA expression in primary LSECs pre-treated with U0126 (10 μM), SP600125 (5 μM), SB202190 (10 μM), or DMSO for 1 h, followed by 100 μM H_2O_2 treatment for 6 h. Experiments in B, C were performed in the presence of hepatocyte-conditioned medium. Data are RT-qPCR results, normalized to the housekeeping gene *Rpl19* and presented as fold change relative to vehicle controls. The dashed line (ut) indicates the mRNA expression of LSECs treated with DMSO or the inhibitors in the absence of H_2O_2. Data are derived from three independent experiments and presented as mean ± SD. Statistical significance: *p<0.05, **p<0.01, ***p<0.001, Student's t-test, one-way ANOVA or two-way ANOVA. FeNTA, ferric nitrilotriacetate; NAC, N-acetyl-L-cysteine.

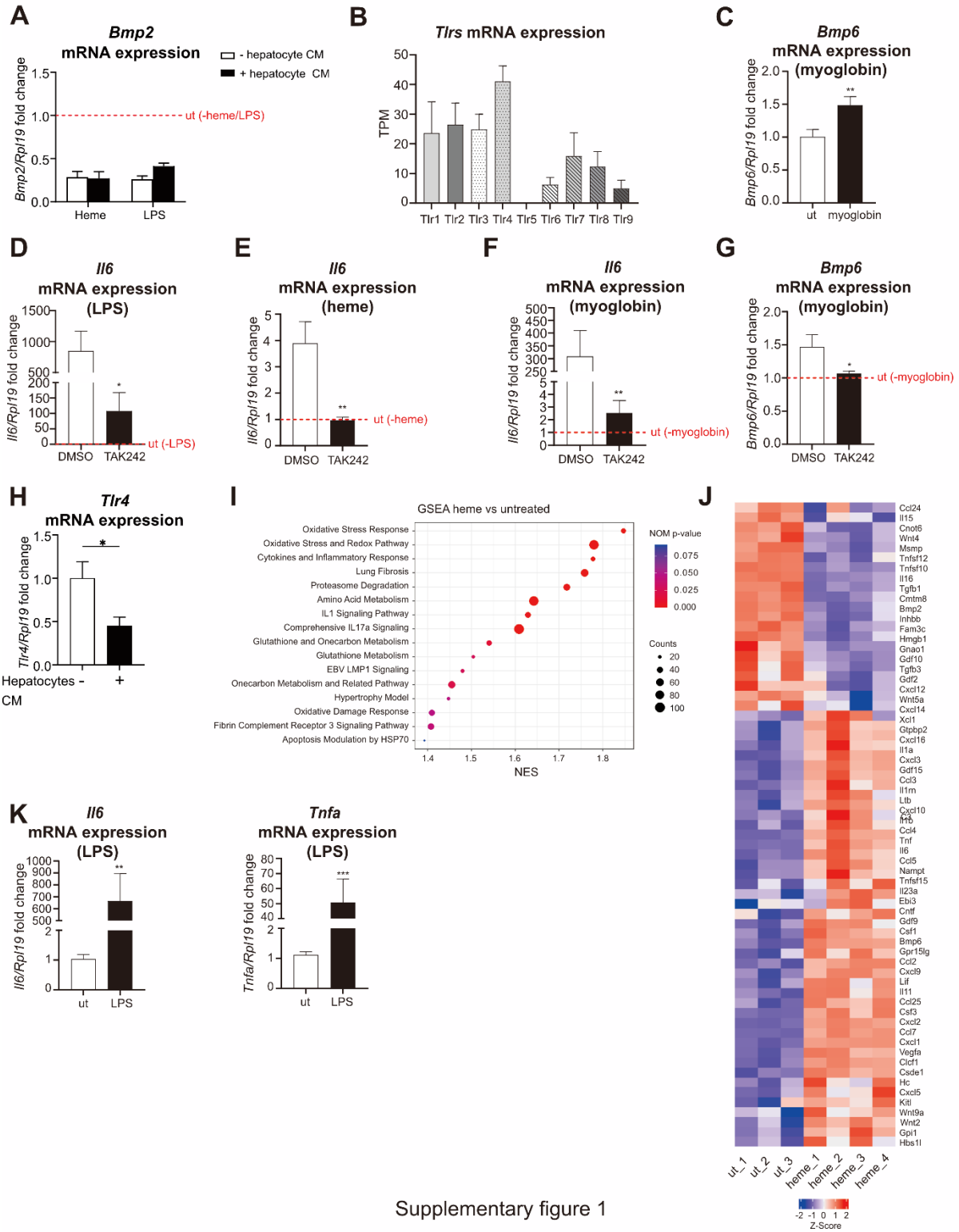

Supplementary figure 1

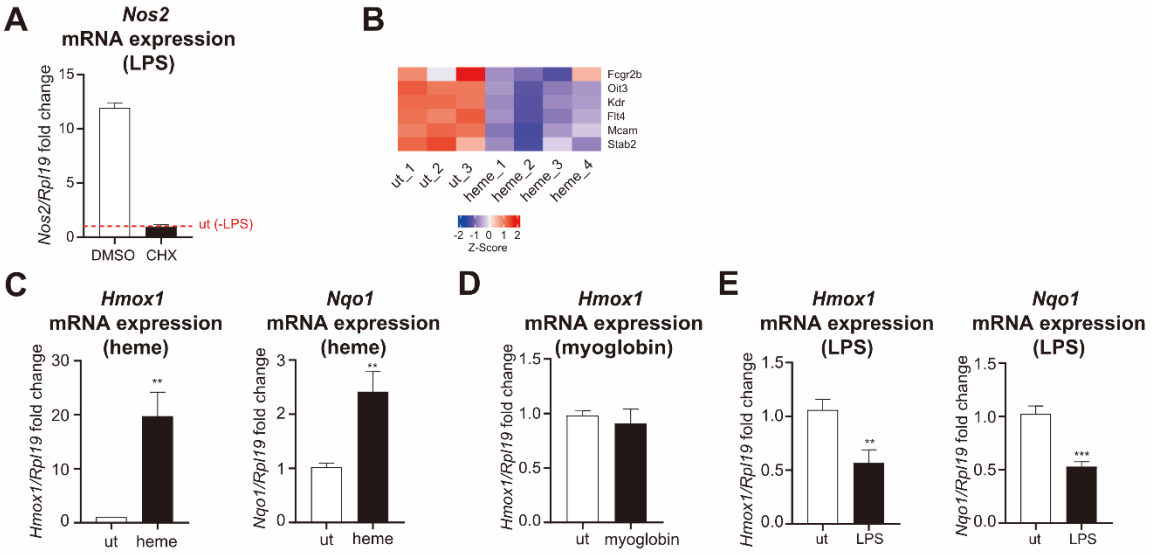

Supplementary figure 2

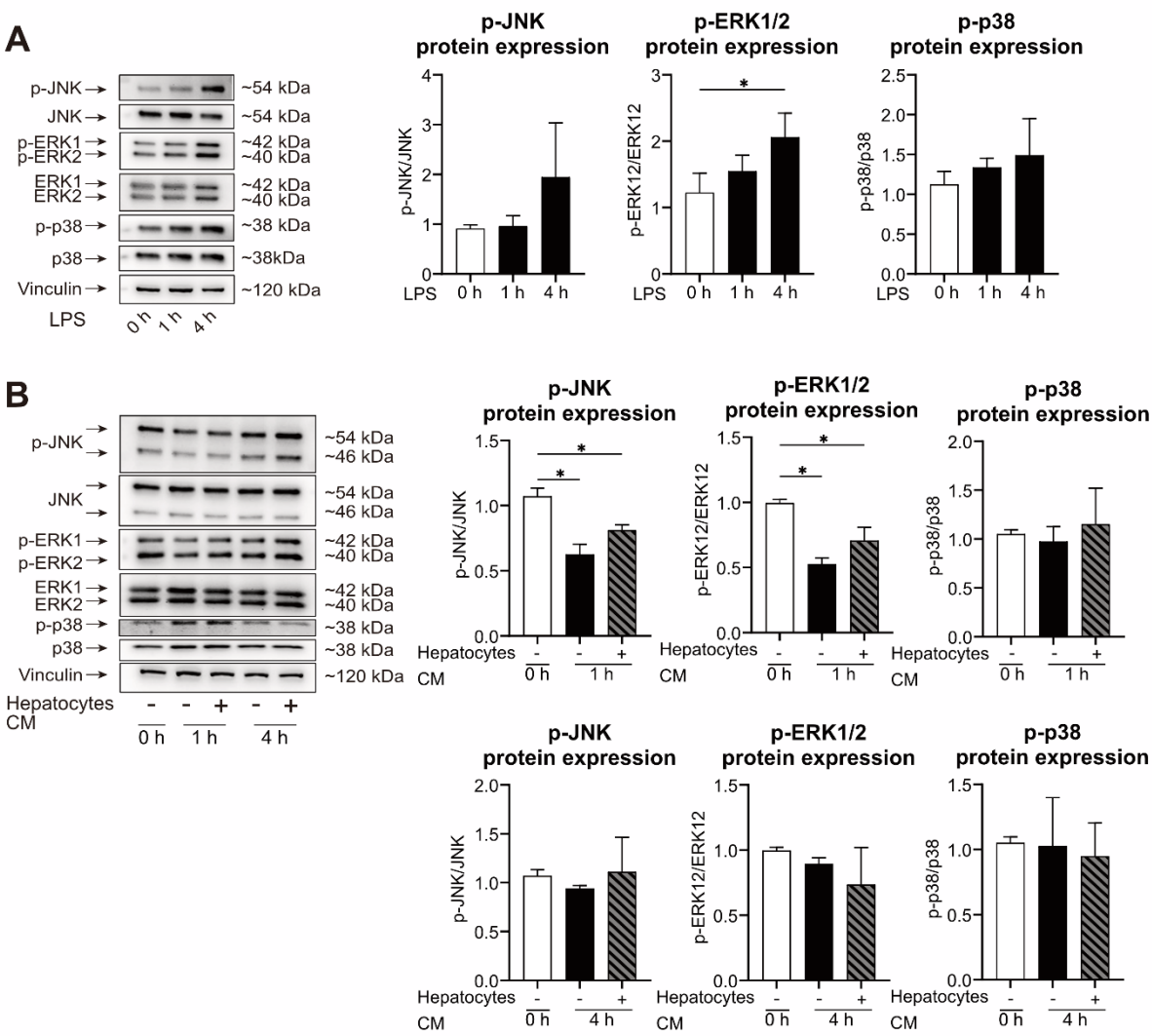

Supplementary figure 3

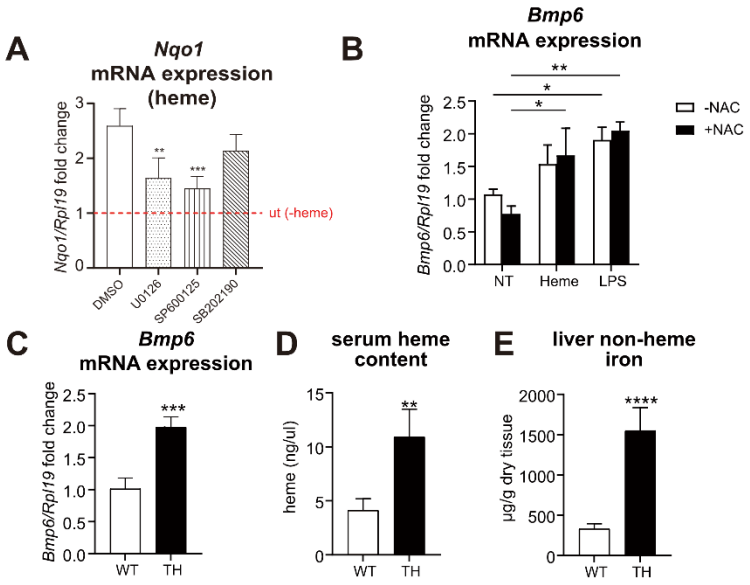

Supplementary figure 4

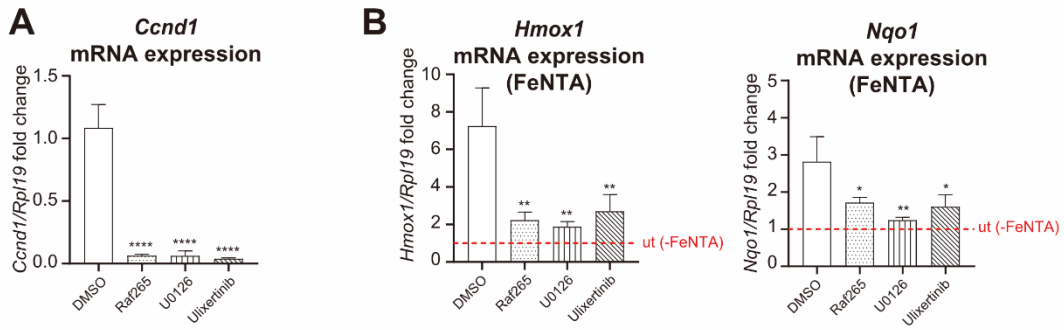

Supplementary figure 5

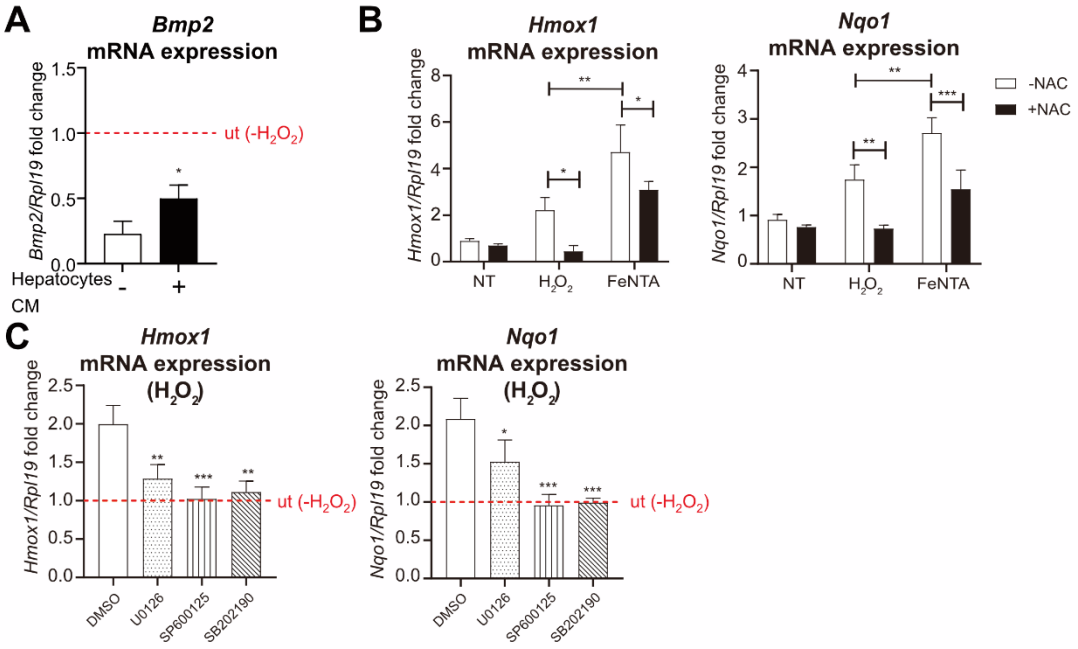

Supplementary figure 6

References

1. Colucci S, Altamura S, Marques O, et al. Liver Sinusoidal Endothelial Cells Suppress Bone Morphogenetic Protein 2 Production in Response to TGFβ Pathway Activation. Hepatology. 2021;74(4):2186-2200.

2. Colucci S, Altamura S, Marques O, et al. Iron-dependent BMP6 Regulation in Liver Sinusoidal Endothelial Cells Is Instructed by Hepatocyte-derived Secretory Signals. Hemasphere. 2022;6(10):e773.

3. Torrance JD, Bothwell TH. A simple technique for measuring storage iron concentrations in formalinised liver samples. S Afr J Med Sci. 1968;33(1):9-11.

4. Sinclair PR, Gorman N, Jacobs JM. Measurement of Heme Concentration. Curr Protoc Toxicol. 1999;00(1):8.3.1-8.3.7.

5. Dobin A, Davis CA, Schlesinger F, et al. STAR: ultrafast universal RNA-seq aligner. Bioinformatics. 2013;29(1):15-21.

6. Müller-Dott S, Tsirvouli E, Vazquez M, et al. Expanding the coverage of regulons from high-confidence prior knowledge for accurate estimation of transcription factor activities. Nucleic Acids Res. 2023;51(20):10934-10949.

7. Subramanian A, Tamayo P, Mootha VK, et al. Gene set enrichment analysis: A knowledge-based approach for interpreting genome-wide expression profiles. Proc Natl Acad Sci U S A. 2005;102(43):15545-15550.

8. Love MI, Huber W, Anders S. Moderated estimation of fold change and dispersion for RNA-seq data with DESeq2. Genome Biol. 2014;15(12):550.